



Measurement of the $pp \rightarrow ZZ$ production cross section and constraints on anomalous triple gauge couplings in four-lepton final states at $\sqrt{s} = 8$ TeV

CMS Collaboration *

CERN, Switzerland

ARTICLE INFO

Article history:

Received 31 May 2014

Received in revised form 20 November 2014

Accepted 30 November 2014

Available online 4 December 2014

Editor: M. Doser

Keywords:

CMS

Physics

Electroweak

ABSTRACT

A measurement of the inclusive ZZ production cross section and constraints on anomalous triple gauge couplings in proton–proton collisions at $\sqrt{s} = 8$ TeV are presented. The analysis is based on a data sample, corresponding to an integrated luminosity of 19.6 fb^{-1} , collected with the CMS experiment at the LHC. The measurements are performed in the leptonic decay modes $ZZ \rightarrow \ell\ell\ell'\ell'$, where $\ell = e, \mu$ and $\ell' = e, \mu, \tau$. The measured total cross section $\sigma(pp \rightarrow ZZ) = 7.7 \pm 0.5 \text{ (stat)}^{+0.5}_{-0.4} \text{ (syst)} \pm 0.4 \text{ (theo)} \pm 0.2 \text{ (lumi)} \text{ pb}$, for both Z bosons produced in the mass range $60 < m_Z < 120 \text{ GeV}$, is consistent with standard model predictions. Differential cross sections are measured and well described by the theoretical predictions. The invariant mass distribution of the four-lepton system is used to set limits on anomalous ZZZ and $ZZ\gamma$ couplings at the 95% confidence level: $-0.004 < f_4^Z < 0.004$, $-0.004 < f_5^Z < 0.004$, $-0.005 < f_4^Y < 0.005$, and $-0.005 < f_5^Y < 0.005$.

© 2014 The Authors. Published by Elsevier B.V. This is an open access article under the CC BY license (<http://creativecommons.org/licenses/by/3.0/>). Funded by SCOAP³.

1. Introduction

The study of diboson production in proton–proton collisions provides an important test of the electroweak sector of the standard model (SM), especially the non-Abelian structure of the SM Lagrangian. In the SM, ZZ production proceeds mainly through quark–antiquark t - and u -channel scattering diagrams. At high-order calculations in QCD, gluon–gluon fusion also contributes via box diagrams with quark loops. There are no tree-level contributions to ZZ production from triple gauge boson vertices in the SM. Anomalous triple gauge couplings (ATGC) ZZZ and $ZZ\gamma$ are introduced using an effective Lagrangian following Ref. [1]. In this parametrization, two ZZZ and two $ZZ\gamma$ couplings are allowed by electromagnetic gauge invariance and Lorentz invariance for on-shell Z bosons and are parametrized by two CP-violating (f_4^Y) and two CP-conserving (f_5^Y) parameters, where $V = (Z, \gamma)$. Nonzero ATGC values could be induced by new physics models such as supersymmetry [2].

Previous measurements of the inclusive ZZ cross section by the CMS Collaboration at the LHC were performed in the $ZZ \rightarrow \ell\ell\ell'\ell'$

decay channels, where $\ell = e, \mu$ and $\ell' = e, \mu, \tau$, with the data corresponding to an integrated luminosity of 5.1 (5.0) fb^{-1} at $\sqrt{s} = 7$ (8) TeV [3,4]. The measured total cross section, $\sigma(pp \rightarrow ZZ)$, is $6.24^{+0.86}_{-0.80} \text{ (stat)}^{+0.41}_{-0.32} \text{ (syst)} \pm 0.14 \text{ (lumi)} \text{ pb}$ at $\sqrt{s} = 7$ TeV and $8.4 \pm 1.0 \text{ (stat)} \pm 0.7 \text{ (syst)} \pm 0.4 \text{ (lumi)} \text{ pb}$ at $\sqrt{s} = 8$ TeV for both Z bosons in the mass range $60 < m_Z < 120 \text{ GeV}$. The ATLAS Collaboration measured a total cross section of $6.7 \pm 0.7 \text{ (stat)}^{+0.4}_{-0.3} \text{ (syst)} \pm 0.3 \text{ (lumi)} \text{ pb}$ [5] using $ZZ \rightarrow \ell\ell\ell\ell$ and $ZZ \rightarrow \ell\ell\nu\nu$ final states with a data sample corresponding to an integrated luminosity of 4.6 fb^{-1} at $\sqrt{s} = 7$ TeV and $66 < m_Z < 116 \text{ GeV}$. Measurements of the ZZ cross sections performed at the Tevatron are summarized in Refs. [6,7]. All measurements are found to agree with the corresponding SM predictions.

Limits on ZZZ and $ZZ\gamma$ ATGCs were set by CMS using the 7 TeV data sample: $-0.011 < f_4^Z < 0.012$, $-0.012 < f_5^Z < 0.012$, $-0.013 < f_4^Y < 0.015$, and $-0.014 < f_5^Y < 0.014$ at 95% confidence level (CL) [3]. Similar limits were obtained by ATLAS [5].

In this analysis, which is based on the full 2012 data set and corresponds to an integrated luminosity of 19.6 fb^{-1} , results are presented for the ZZ inclusive and differential cross sections as well as limits for the ZZZ and $ZZ\gamma$ ATGCs. The cross sections are measured for both Z bosons in the mass range $60 < m_Z < 120 \text{ GeV}$; contributions from virtual photon exchange are included.

* E-mail address: cms-publication-committee-chair@cern.ch.

2. The CMS detector and simulation

The CMS detector is described in detail elsewhere [8]; the key components for this analysis are summarized here. The CMS experiment uses a right-handed coordinate system, with the origin at the nominal interaction point, the x axis pointing to the center of the LHC ring, the y axis pointing up (perpendicular to the plane of the LHC ring), and the z axis along the counterclockwise-beam direction. The polar angle θ is measured from the positive z axis and the azimuthal angle ϕ is measured in the x - y plane. The magnitude of the transverse momentum is $p_T = \sqrt{p_x^2 + p_y^2}$. A superconducting solenoid is located in the central region of the CMS detector, providing an axial magnetic field of 3.8T parallel to the beam direction. A silicon pixel and strip tracker, a crystal electromagnetic calorimeter (ECAL), and a brass and scintillator hadron calorimeter are located within the solenoid and cover the absolute pseudorapidity range $|\eta| < 3.0$, where pseudorapidity is defined as $\eta = -\ln[\tan(\theta/2)]$. The ECAL barrel region (EB) covers $|\eta| < 1.479$ and two endcap regions (EE) cover $1.479 < |\eta| < 3.0$. A quartz-fiber Cherenkov calorimeter extends the coverage up to $|\eta| < 5.0$. Gas ionization muon detectors are embedded in the steel flux-return yoke outside the solenoid. A first level of the CMS trigger system, composed of custom hardware processors, is designed to select events of interest in less than 4 μ s using information from the calorimeters and muon detectors. A high-level-trigger processor farm reduces the event rate from 100 kHz delivered by the first level trigger to a few hundred hertz.

Several Monte Carlo (MC) event generators are used to simulate the signal and background contributions. The $q\bar{q} \rightarrow ZZ$ process is generated at next-to-leading order (NLO) with POWHEG 2.0 [9–11] or at leading-order (LO) with SHERPA [12]. The $gg \rightarrow ZZ$ process is simulated with gg2zz [13] at LO. Other diboson processes (WZ , $Z\gamma$) and the $Z +$ jets samples are generated at LO with MADGRAPH 5 [14]. Events from $t\bar{t}$ production are generated at NLO with POWHEG. The PYTHIA 6.4 [15] package is used for parton showering, hadronization, and the underlying event simulation. The default set of parton distribution functions (PDF) used for LO generators is CTEQ6L [16], whereas CT10 [17] is used for NLO generators. The ZZ yields from simulation are scaled according to the theoretical cross sections calculated with MCFM 6.0 [18] at NLO for $qq \rightarrow ZZ$ and at LO for $gg \rightarrow ZZ$ with the MSTW2008 PDF [19] with renormalization and factorization scales set to $\mu_R = \mu_F = 91.2$ GeV. The τ -lepton decays are simulated with TAUOLA [20]. For all processes, the detector response is simulated using a detailed description of the CMS detector based on the GEANT4 package [21], and event reconstruction is performed with the same algorithms that are used for data. The simulated samples include multiple interactions per bunch crossing (pileup), such that the pileup distribution matches that of data, with an average value of about 21 interactions per bunch crossing.

3. Event reconstruction

A complete reconstruction of the individual particles emerging from each collision event is obtained via a particle-flow (PF) technique [22,23], which uses the information from all CMS sub-detectors to identify and reconstruct individual particles in the collision event. The particles are classified into mutually exclusive categories: charged hadrons, neutral hadrons, photons, muons, and electrons.

Electrons are reconstructed within the geometrical acceptance, $|\eta^e| < 2.5$, and for transverse momentum $p_T^e > 7$ GeV. The reconstruction combines the information from clusters of energy deposits in the ECAL and the trajectory in the tracker [24]. Particle

trajectories in the tracker volume are reconstructed using a modeling of the electron energy loss and fitted with a Gaussian sum filter [25]. The contribution of the ECAL energy deposits to the electron transverse momentum measurement and its uncertainty are determined via a multivariate regression approach. Electron identification relies on a multivariate technique that combines observables sensitive to the amount of bremsstrahlung along the electron trajectory, the geometrical and momentum matching between the electron trajectory and associated clusters, as well as shower shape observables.

Muons are reconstructed within $|\eta^\mu| < 2.4$ and for $p_T^\mu > 5$ GeV [26]. The reconstruction combines information from both the silicon tracker and the muon detectors. The PF muons are selected from among the reconstructed muon track candidates by applying requirements on the track components in the muon system and matching with minimum ionizing particle energy deposits in the calorimeters.

For τ leptons, two principal decay modes are distinguished: a leptonic mode, τ_ℓ , with a final state including either an electron or a muon, and a hadronic mode, τ_h , with a final state including hadrons. The PF particles are used to reconstruct τ_h with the “hadron-plus-strip” algorithm [27], which optimizes the reconstruction and identification of specific τ_h decay modes. The π^0 components of the τ_h decays are first reconstructed and then combined with charged hadrons to reconstruct the τ_h decay modes. Cases where τ_h includes three charged hadrons are also included. The missing transverse energy that is associated with neutrinos from τ decays is ignored in the reconstruction. The τ_h candidates in this analysis are required to have $|\eta^{\tau_h}| < 2.3$ and $p_T^{\tau_h} > 20$ GeV.

The isolation of individual electrons or muons is measured relative to their transverse momentum p_T^ℓ , by summing over the transverse momenta of charged hadrons and neutral particles in a cone with $\Delta R = \sqrt{(\Delta\eta)^2 + (\Delta\phi)^2} = 0.4$ around the lepton direction at the interaction vertex:

$$R_{\text{iso}}^\ell = \left(\sum p_T^{\text{charged}} + \text{MAX}\left[0, \sum p_T^{\text{neutral}} + \sum p_T^\gamma - \rho \times A_{\text{eff}} \right] \right) / p_T^\ell. \quad (1)$$

The $\sum p_T^{\text{charged}}$ is the scalar sum of the transverse momenta of charged hadrons originating from the primary vertex. The primary vertex is chosen as the vertex with the highest sum of p_T^2 of its constituent tracks. The $\sum p_T^{\text{neutral}}$ and $\sum p_T^\gamma$ are the scalar sums of the transverse momenta for neutral hadrons and photons, respectively. The average transverse-momentum flow density ρ is calculated in each event using a “jet area” [28], where ρ is defined as the median of the $p_T^{\text{jet}}/A_{\text{jet}}$ distribution for all pileup jets in the event. The effective area A_{eff} is the geometric area of the isolation cone times an η -dependent correction factor that accounts for the residual dependence of the isolation on pileup. Electrons and muons are considered isolated if $R_{\text{iso}}^\ell < 0.4$. Allowing τ leptons in the final state increases the background contamination, therefore tighter isolation requirements are imposed for electrons and muons in $ZZ \rightarrow \ell\ell\tau\tau$ decays: $R_{\text{iso}}^\ell < 0.25$ for $Z \rightarrow \tau_\ell^+\tau_\ell^-$, and $R_{\text{iso}}^e < 0.1$ for $Z \rightarrow \tau_e\tau_h$, and $R_{\text{iso}}^\mu < 0.15$ for $\tau_\mu\tau_h$.

The isolation of the τ_h is calculated as the scalar sum of the transverse momenta of the charged hadrons and neutral particles in a cone of $\Delta R = 0.5$ around the τ_h direction reconstructed at the interaction vertex. The τ_h isolation includes a correction for pileup effects, which is based on the scalar sum of transverse momenta of charged particles not associated with the primary vertex in a cone of $\Delta R = 0.8$ about the τ_h candidate direction (p_T^{PU}). The isolation variable is defined as:

$$I^{\text{PF}} = \left(\sum p_{\text{T}}^{\text{charged}} + \text{MAX} \left[0, \sum p_{\text{T}}^{\text{neutral}} + \sum p_{\text{T}}^{\gamma} - f \times p_{\text{T}}^{\text{PU}} \right] \right), \quad (2)$$

where the scale factor of $f = 0.0729$, which is used in estimating the contribution to the isolation sum from neutral hadrons and photons, accounts for the difference in the neutral and charged contributions and in the cone sizes. Two standard working points are defined based on the value of the isolation sum corrected for the pileup contribution: $I^{\text{PF}} < 1(8)$ GeV for final states including one (two) τ_h candidates.

The electron and muon pairs from Z-boson decays are required to originate from the primary vertex. This is ensured by demanding that the significance of the three-dimensional impact parameter relative to the event vertex, SIP_{3D} , satisfies $SIP_{3D} = |\frac{IP}{\sigma_{IP}}| < 4$ for each lepton. The IP is the distance of closest approach of the lepton track to the primary vertex and σ_{IP} is its associated uncertainty.

The combined efficiencies of reconstruction, identification, and isolation of primary electrons or muons are measured in data using a “tag-and-probe” technique [29] applied to an inclusive sample of Z events. The measurements are performed in bins of p_{T}^{ℓ} and $|\eta^{\ell}|$. The efficiency for selecting electrons in the ECAL barrel (endcaps) is about 70% (60%) for $7 < p_{\text{T}}^e < 10$ GeV, 85% (77%) at $p_{\text{T}}^e \simeq 10$ GeV, and 95% (89%) for $p_{\text{T}}^e \geq 20$ GeV. It is about 85% in the transition region between the ECAL barrel and endcaps ($1.44 < |\eta| < 1.57$), averaging over the whole p_{T} range. The muons are reconstructed and identified with an efficiency greater than $\sim 98\%$ in the full $|\eta^{\mu}| < 2.4$ range. The τ_h reconstruction efficiency is approximately 50% [27].

Final-state radiation (FSR) may affect the measured four-momentum of the leptons if it is not properly included in the reconstruction. For electrons, a significant portion of the FSR photons is included in the reconstructed energy because of the size of the electromagnetic clusters, but for muons additional treatment of the FSR photons is important. All photons reconstructed within $|\eta^{\mu}| < 2.4$ are considered as possible FSR candidates if they have a transverse momentum $p_{\text{T}}^{\gamma} > 2(4)$ GeV and are found within $\Delta R < 0.07$ ($0.07 < \Delta R < 0.5$) from the closest selected lepton candidate and are isolated. The photon isolation observable R_{iso}^{γ} is the sum of the transverse momenta of charged hadrons, neutral hadrons, and photons in a cone of $\Delta R = 0.3$ around the candidate photon direction, divided by p_{T}^{γ} . Isolated photons must satisfy $R_{\text{iso}}^{\gamma} < 1$. The recovered FSR photon is included in the lepton four-momentum and the lepton isolation is then recalculated without it.

The performance of the FSR selection algorithm has been determined using simulated samples, and the rate is verified with the Z and ZZ events in data. The photons within the acceptance for the FSR selection are reconstructed with an efficiency of about 50% and with a mean purity of 80%. The FSR photons are recovered in 0.5(5)% of inclusive Z events with electron (muon) pairs.

4. Event selection

The data sample used in this analysis is selected by the trigger system, which requires the presence of a pair of electrons or muons, or a triplet of electrons. Triggers requiring an electron and a muon are also used. For the double-lepton triggers, the highest p_{T} and the second-highest p_{T} leptons are required to have p_{T} greater than 17 and 8 GeV, respectively, while for the triple-electron trigger the thresholds are 15, 8, and 5 GeV. The trigger efficiency for ZZ events within the acceptance of this analysis is greater than 98%. The use of the triple-electron trigger with a looser p_{T} requirement helps to recover 1–2% of the signal events, while for muons such contribution was found to be negligible.

In selected ZZ events, the Z candidate with the mass closest to the Z-boson mass is denoted Z_1 and the other one, Z_2 . The selection is designed to give mutually exclusive sets of signal candidates first selecting ZZ decays to $4e$, 4μ , and $2e2\mu$, in the following denoted $\ell\ell''\ell''$; these events are not considered in $ZZ \rightarrow \ell\ell\tau\tau$ channel. The leptons are identified and isolated as described in Section 3. When building the Z candidates, the FSR photons are kept if $|m_{\ell\ell\gamma} - m_Z| < |m_{\ell\ell} - m_Z|$ and $m_{\ell\ell\gamma} < 100$ GeV. In the following, the presence of the photons in the $\ell\ell''\ell''$ kinematics is implicit. The leptons constituting a Z candidate are required to be the same flavor and to have opposite charges ($\ell^+\ell^-$). The pair is retained if it satisfies $60 < m_Z < 120$ GeV. If more than one Z_2 candidate satisfies all criteria, the ambiguity is resolved by choosing the pair of leptons with the highest scalar sum of p_{T} . Among the four selected leptons forming the Z_1 and the Z_2 , at least one should have $p_{\text{T}} > 20$ GeV and another one should have $p_{\text{T}} > 10$ GeV. These p_{T} thresholds ensure that the selected events have leptons with p_{T} values on the high-efficiency plateau for the trigger.

For the $\ell\ell\tau\tau$ final state, events are required to have one $Z_1 \rightarrow \ell^+\ell^-$ candidate with $p_{\text{T}} > 20$ GeV for one of the leptons and $p_{\text{T}} > 10$ GeV for the other lepton, and a $Z_2 \rightarrow \tau^+\tau^-$, with τ decaying into τ_e , τ_{μ} , or τ_h . The leptons from the τ_{ℓ} decays are required to have $p_{\text{T}}^{\tau_{\ell}} > 10$ GeV. The τ_h candidates are required to have $p_{\text{T}}^{\tau_h} > 20$ GeV. The FSR recovery is not applied to the $\ell\ell\tau\tau$ final states, since it does not improve the mass reconstruction. The invariant mass of the reconstructed Z_1 is required to satisfy $60 < m_{\ell\ell} < 120$ GeV, and that of the Z_2 to satisfy $m_{\min} < m_{\tau\tau} < 90$ GeV, where $m_{\min} = 20$ GeV for $Z_2 \rightarrow \tau_e\tau_{\mu}$ final states and 30 GeV for all others.

5. Background estimation

The lepton identification and isolation requirements described in Section 3 significantly suppress all background contributions, and the remnant portion of them arise mainly from the Z and WZ production in association with jets, as well as $t\bar{t}$. In all these cases, a jet or a non-prompt lepton is misidentified as an isolated e, μ , τ_h , τ_e , or τ_{μ} . Leptons produced in the decay of Z bosons are referred to as prompt leptons; leptons from e.g. heavy meson decays are non-prompt. The requirements to eliminate non-prompt leptons also remove hadrons that appear to be leptons.

To estimate the expected number of background events in the signal region, control data samples are defined for each lepton flavor combination $\ell'\ell'$. The e and τ_e , and μ and τ_{μ} are considered as different flavors, since they originate from different particles.

The control data samples for the background estimate are obtained by selecting events containing Z_1 , which passes all selection requirements, and two additional lepton candidates $\ell'\ell'$. The additional lepton pair must have opposite charge and matching flavor ($e^{\pm}e^{\mp}$, $\mu^{\pm}\mu^{\mp}$, $\tau^{\pm}\tau^{\mp}$). Control data samples enriched with $Z + X$ events, where X stands for $b\bar{b}$, $c\bar{c}$, gluon, or light quark jets, are obtained by requiring that both additional leptons pass only relaxed identification criteria and are required to be not isolated. By requiring one of the additional leptons to pass the full selection requirements, one obtains data samples enriched with WZ events and significant number of $t\bar{t}$ events. The expected number of background events in the signal region for each flavor pair is obtained by scaling the number of observed $Z_1 + \ell'\ell'$ events by the lepton misidentification probability and combining the results for $Z + X$ and WZ , $t\bar{t}$ control regions together. The procedure is identical for all lepton flavors.

The misidentification probability, i.e., the probability for a lepton candidate that passes the relaxed requirements to pass the full selection, is measured separately for each flavor from a sample of $Z_1 + \ell_{\text{candidate}}$ events with a relaxed identification and no isolation

Table 1

The expected yields of ZZ and background events, as well as their sum (“Total expected”) are compared with the observed yields for each decay channel. The statistical and systematic uncertainties are also shown.

Decay channel	Expected ZZ yield	Background	Total expected	Observed
4e	$55.28 \pm 0.25 \pm 7.64$	$2.16 \pm 0.26 \pm 0.88$	$57.44 \pm 0.37 \pm 7.69$	54
4μ	$77.32 \pm 0.29 \pm 10.08$	$1.19 \pm 0.36 \pm 0.48$	$78.51 \pm 0.49 \pm 10.09$	75
$2e2\mu$	$136.09 \pm 0.59 \pm 17.50$	$2.35 \pm 0.34 \pm 0.93$	$138.44 \pm 0.70 \pm 17.52$	148
$ee\tau_h\tau_h$	$2.46 \pm 0.03 \pm 0.32$	$3.46 \pm 0.34 \pm 1.04$	$5.92 \pm 0.36 \pm 1.15$	10
$\mu\mu\tau_h\tau_h$	$2.80 \pm 0.03 \pm 0.34$	$3.89 \pm 0.37 \pm 1.17$	$6.69 \pm 0.39 \pm 1.30$	10
$ee\tau_e\tau_h$	$2.79 \pm 0.03 \pm 0.36$	$3.87 \pm 1.26 \pm 1.16$	$6.66 \pm 1.34 \pm 1.29$	9
$\mu\mu\tau_e\tau_h$	$2.87 \pm 0.03 \pm 0.37$	$1.49 \pm 0.67 \pm 0.60$	$4.36 \pm 0.71 \pm 0.73$	2
$ee\tau_\mu\tau_h$	$3.27 \pm 0.03 \pm 0.42$	$1.47 \pm 0.41 \pm 0.44$	$4.74 \pm 0.43 \pm 0.63$	2
$\mu\mu\tau_\mu\tau_h$	$3.81 \pm 0.03 \pm 0.50$	$1.55 \pm 0.43 \pm 0.46$	$5.36 \pm 0.46 \pm 0.70$	5
$ee\tau_e\tau_\mu$	$2.23 \pm 0.03 \pm 0.29$	$3.04 \pm 1.32 \pm 1.50$	$5.27 \pm 1.40 \pm 1.61$	4
$\mu\mu\tau_e\tau_\mu$	$2.41 \pm 0.03 \pm 0.32$	$0.74 \pm 0.51 \pm 0.37$	$3.15 \pm 0.54 \pm 0.51$	5
Total $\ell\ell\tau\tau$	$22.65 \pm 0.05 \pm 2.94$	$19.51 \pm 2.15 \pm 5.85$	$42.16 \pm 2.28 \pm 6.87$	47

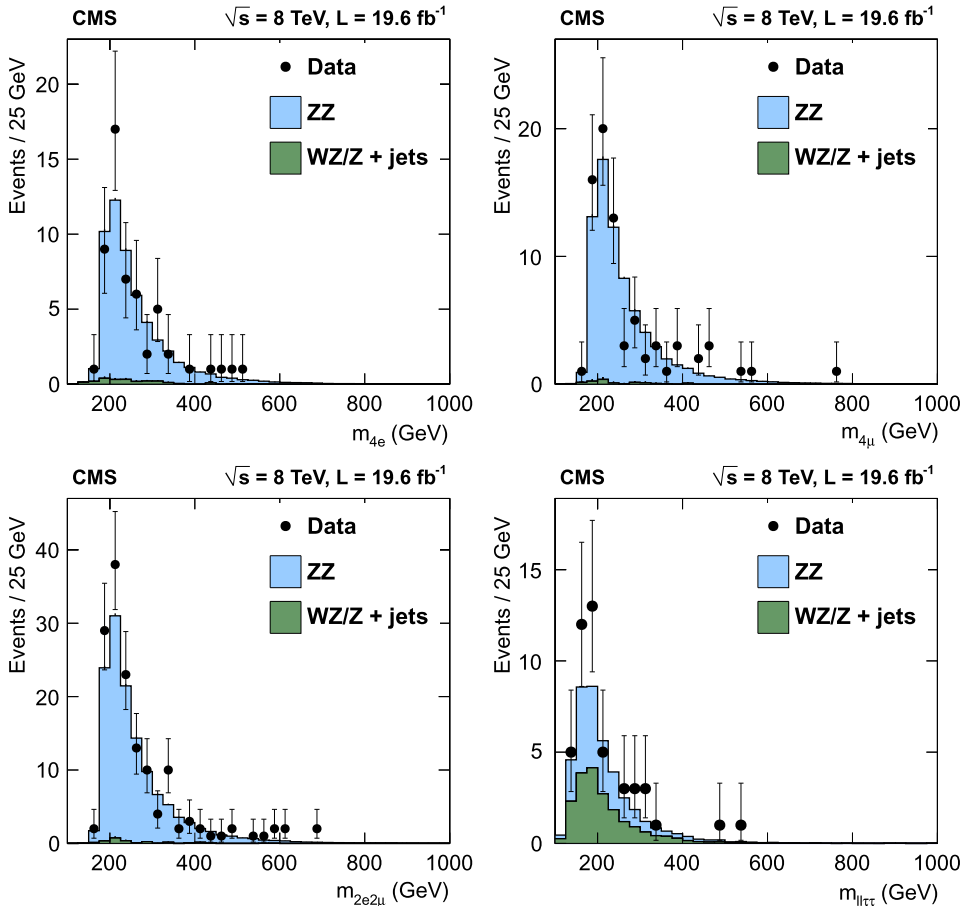


Fig. 1. Distribution of the reconstructed four-lepton mass for the (upper left) 4e, (upper right) 4μ, (lower left) 2e2μ, and (lower right) combined $\ell\ell\tau\tau$ decay channels. The data sample corresponds to an integrated luminosity of 19.6 fb^{-1} . Points represent the data, the shaded histograms labeled ZZ represent the POWHEG+GG2ZZ+PYTHIA predictions for ZZ signal, the histograms labeled WZ/Z + jets show the background, which is estimated from data, as described in the text.

requirements on the $\ell_{\text{candidate}}$. The misidentification probability for each lepton flavor is defined as the ratio of the number of leptons that pass the final isolation and identification requirements to the total number of leptons in the sample. It is measured in bins of lepton p_T and η . The contamination from WZ events, which may lead to an overestimate of the misidentification probability because of the presence of genuine isolated leptons, is suppressed by requiring that the measured missing transverse energy is less than 25 GeV.

The estimated background contributions to the signal region are summarized in Table 1. The procedure excludes a possible double

counting due to Z + X events that can be found in the WZ control region. A correction for the small contribution of ZZ events in the control region is applied based on MC simulation. The predicted background yield has a small effect on the ZZ cross section measurement in the $\ell\ell\ell''\ell''$ channels, but is comparable to the signal yield for the case of $\ell\ell\tau\tau$.

6. Systematic uncertainties

The systematic uncertainties for trigger efficiency (1.5%) are evaluated from data. The uncertainties arising from lepton identi-

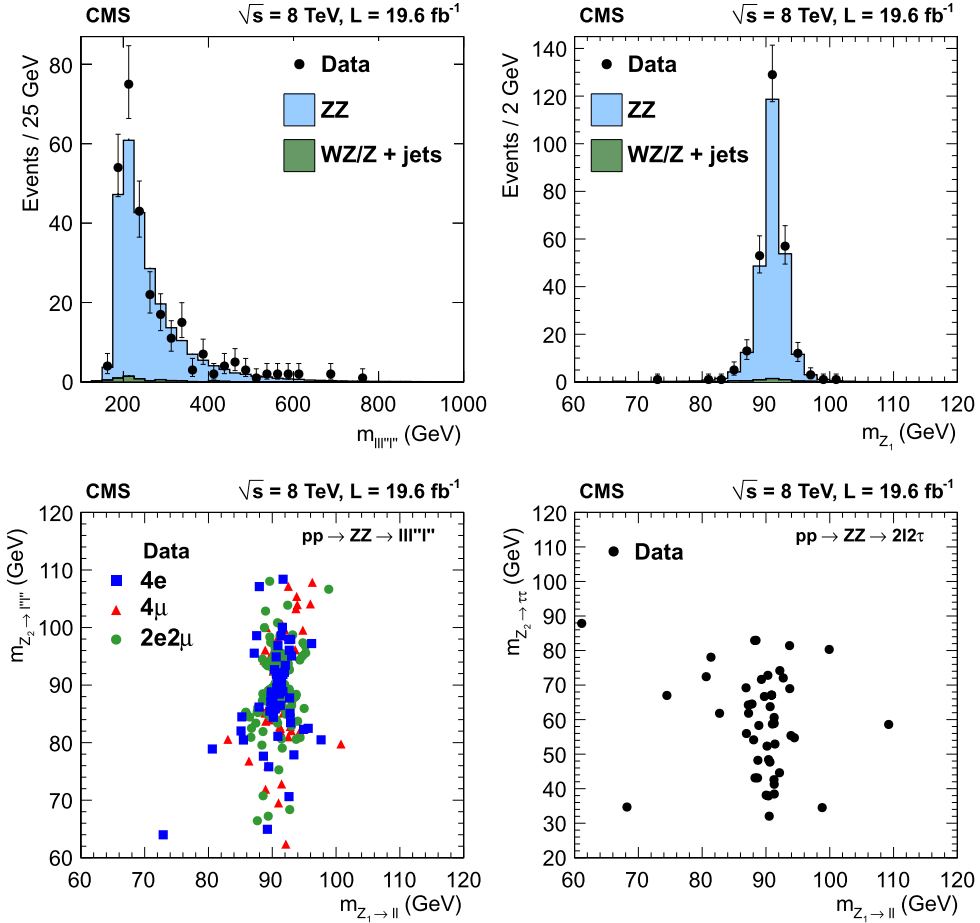


Fig. 2. (upper left) Distribution of the reconstructed four-lepton mass for the sum of the 4e, 4μ, and 2e2μ decay channels. (upper right) Reconstructed Z_1 mass. The correlation between the reconstructed Z_1 and Z_2 masses for the (lower left) combined 4e, 4μ, and 2e2μ final states and (lower right) for $\ell\ell\tau\tau$ final states. Points represent the data, the shaded histograms labeled ZZ represent the POWHEG+GG2ZZ+PYTHIA predictions for ZZ signal, the histograms labeled WZ/Z + jets show background, which is estimated from data, as described in the text.

fication and isolation are 1–2% for muons and electrons, and 6–7% for τ_h . The uncertainty in the LHC integrated luminosity of the data sample is 2.6% [30].

Theoretical uncertainties in the $ZZ \rightarrow \ell\ell\ell'\ell'$ acceptance are evaluated using MCFM and by varying the renormalization and factorization scales, up and down, by a factor of two with respect to the default values $\mu_R = \mu_F = m_Z$. The variations in the acceptance are 0.1% (NLO $q\bar{q} \rightarrow ZZ$) and 0.4% ($gg \rightarrow ZZ$), and can be neglected. Uncertainties related to the choice of the PDF and the strong coupling constant α_s are evaluated following the PDF4LHC [31] prescription and using CT10, MSTW08, and NNPDF [32] PDF sets and found to be 4% (NLO $q\bar{q} \rightarrow ZZ$) and 5% ($gg \rightarrow ZZ$).

The uncertainties in $Z + \text{jets}$, $WZ + \text{jets}$, and $t\bar{t}$ yields reflect the uncertainties in the measured values of the misidentification rates and the limited statistics of the control regions in the data, and vary between 20% and 70%.

The uncertainty in the unfolding procedure discussed in Section 7 arises from differences between SHERPA and POWHEG for the unfolding factors (2–3%), from scale and PDF uncertainties (4–5%), and from experimental uncertainties (4–5%).

7. The ZZ cross section measurement

The measured and expected event yields for all decay channels are summarized in Table 1. The recently discovered Higgs particle with the mass of 125 GeV does not contribute to this analysis as background because of the phase space selection requirements.

The reconstructed four-lepton invariant mass distributions for the 4e, 4μ, 2e2μ, and combined $\ell\ell\tau\tau$ decay channels are shown in Fig. 1. The shape of the background is taken from data. The reconstructed four-lepton invariant mass distribution for the combined 4e, 4μ, and 2e2μ channels is shown in Fig. 2 (upper left). Fig. 2 (upper right) presents the invariant mass of the Z_1 candidates. Figs. 2 (lower left) and (lower right) show the correlation between the reconstructed Z_1 and Z_2 masses for (lower left) 4e, 4μ, and 2e2μ and for (lower right) $\ell\ell\tau\tau$ final states. The data are well reproduced by the signal simulation and with background predictions estimated from data.

The measured yields are used to evaluate the total ZZ production cross section. The signal acceptance is evaluated from simulation and corrected for each individual lepton flavor in bins of p_T and η using factors obtained with the “tag-and-probe” technique. The requirements on p_T and η for the particles in the final state reduce the full possible phase space of the $ZZ \rightarrow 4\ell$ measurement by a factor within a range of 0.56–0.59 for the 4e, 4μ, and 2e2μ, depending on the final state, and by a factor of 0.18–0.21 for the $\ell\ell\tau\tau$ final states, with respect to all events generated in the mass window $60 < m_{Z_1}, m_{Z_2} < 120$ GeV. The branching fraction for $Z \rightarrow \ell'\ell'$ is $(3.3658 \pm 0.0023)\%$ for each lepton flavor [33].

To include all final states in the cross section calculation, a simultaneous fit to the number of observed events in all decay channels is performed. The likelihood is written as a combination of individual channel likelihoods for the signal and background

Table 2

The total ZZ production cross section as measured in each decay channel and for the combination of all channels.

Decay channel	Total cross section, pb
4e	$7.2^{+1.0}_{-0.9}$ (stat) $^{+0.6}_{-0.5}$ (syst) ± 0.4 (theo) ± 0.2 (lumi)
4 μ	$7.3^{+0.8}_{-0.8}$ (stat) $^{+0.6}_{-0.5}$ (syst) ± 0.4 (theo) ± 0.2 (lumi)
2e2 μ	$8.1^{+0.7}_{-0.6}$ (stat) $^{+0.6}_{-0.5}$ (syst) ± 0.4 (theo) ± 0.2 (lumi)
$\ell\ell\tau\tau$	$7.7^{+2.1}_{-1.9}$ (stat) $^{+2.0}_{-1.8}$ (syst) ± 0.4 (theo) ± 0.2 (lumi)
Combined	7.7 ± 0.5 (stat) $^{+0.5}_{-0.4}$ (syst) ± 0.4 (theo) ± 0.2 (lumi)

hypotheses, with systematical uncertainties used as nuisance parameters in the fit. Each τ -lepton decay mode, listed in Table 1, is treated as a separate channel.

Table 2 lists the total cross section obtained from each individual decay channel as well as the total cross section based on the combination of all channels. The measured cross section agrees with the theoretical value of 7.7 ± 0.6 pb calculated with MCFM 6.0. In this calculation, the contribution from $q\bar{q} \rightarrow ZZ$ is

obtained at NLO, while the smaller contribution (approximately 6%) from $gg \rightarrow ZZ$ is obtained at LO. The MSTW2008 PDF is used and the renormalization and factorization scales set to $\mu_R = \mu_F = 91.2$ GeV.

The measurement of the differential cross sections is an important part of this analysis, since it provides detailed information about ZZ kinematics. Three decay channels, 4e, 4 μ , and 2e2 μ , are combined, since their kinematic distributions are the same; the $\ell\ell\tau\tau$ channel is not included. The observed yields are unfolded using the method described in Ref. [34].

The differential distributions normalized to the fiducial cross sections are presented in Figs. 3 and 4 for the combination of the 4e, 4 μ , and 2e2 μ decay channels. The fiducial cross section definition includes p_T^ℓ and $|\eta^\ell|$ selections on each lepton, and the 60–120 GeV mass requirement, as described in Section 4. Fig. 3 shows the differential cross sections in bins of p_T for: (upper left) the highest- p_T lepton in the event, (upper right) the Z_1 , and (lower left) the ZZ system. Fig. 3 (lower left) shows the normalized $d\sigma/dm_{ZZ}$ distribution. The data are corrected for background contributions and compared with the theoretical predictions from

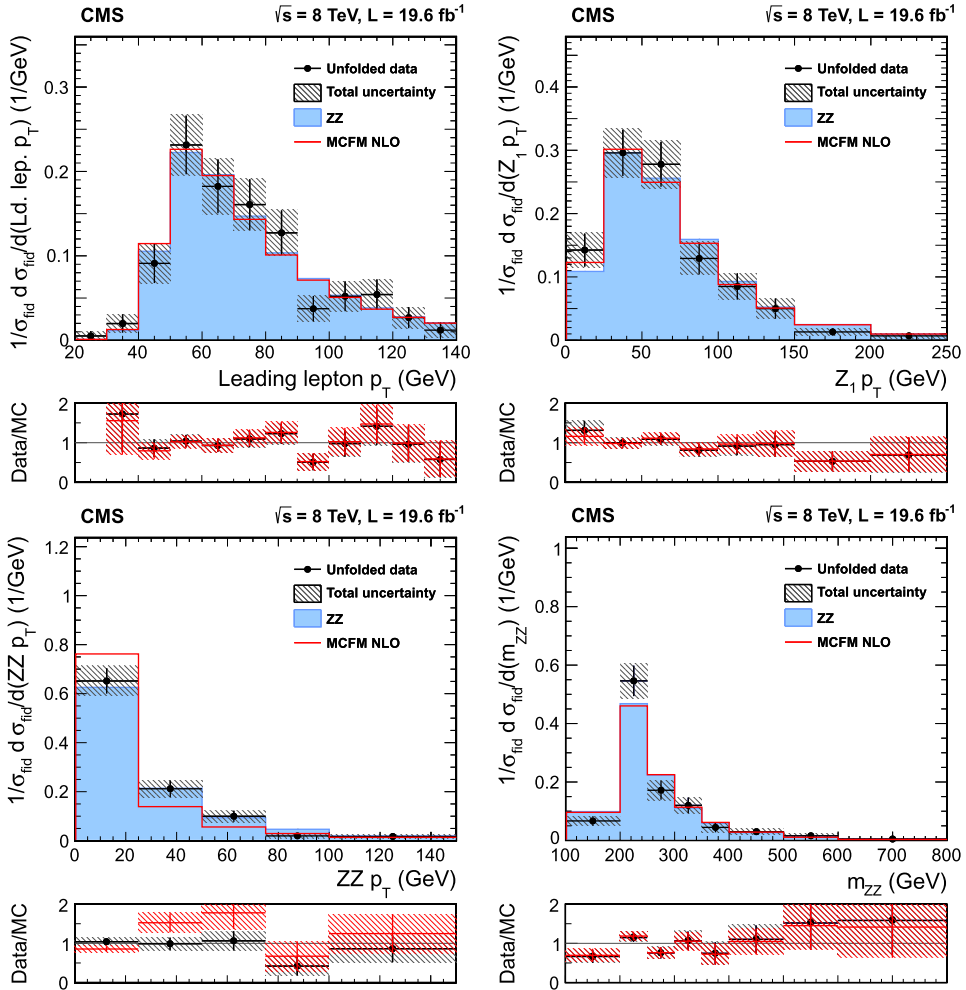


Fig. 3. Differential cross sections normalized to the fiducial cross section for the combined 4e, 4 μ , and 2e2 μ decay channels as a function of p_T for (upper left) the highest p_T lepton in the event, (upper right) the Z_1 , and (lower left) the ZZ system. Figure (lower right) shows the normalized $d\sigma/dm_{ZZ}$ distribution. Points represent the data, and the shaded histograms labeled ZZ represent the POWHEG+CG2ZZ+PYTHIA predictions for ZZ signal, while the solid curves correspond to results of the MCFM calculations. The bottom part of each subplot represents the ratio of the measured cross section to the expected one from POWHEG+CG2ZZ+PYTHIA (black crosses with solid symbols) and MCFM (red crosses). The shaded areas on all the plots represent the full uncertainties calculated as the quadrature sum of the statistical and systematic uncertainties, whereas the crosses represent the statistical uncertainties only. (For interpretation of the references to color in this figure legend, the reader is referred to the web version of this article.)

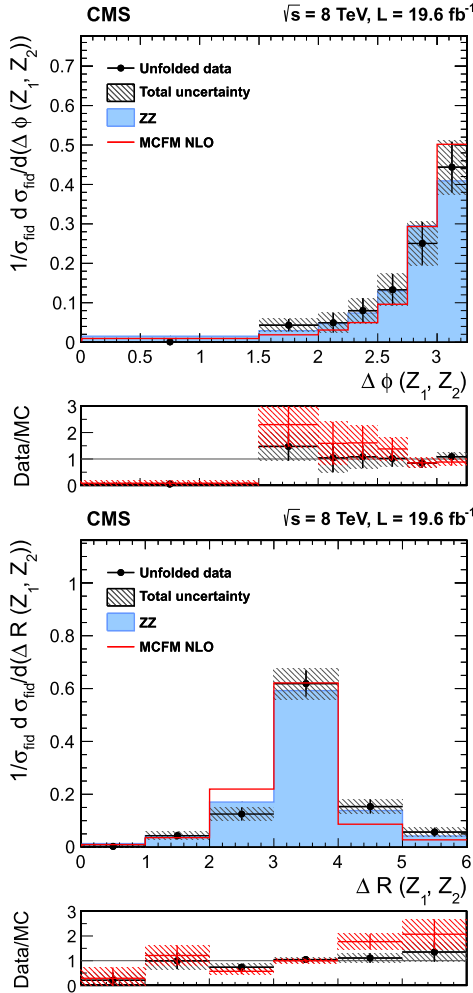


Fig. 4. Differential cross section normalized to the fiducial cross section for the combined 4e, 4 μ , and 2e2 μ decay channels as a function of (top) azimuthal separation of the two Z bosons and (bottom) ΔR between the Z-bosons. Points represent the data, and the shaded histograms labeled ZZ represent the POWHEG+GG2ZZ+PYTHIA predictions for ZZ signal, while the solid curves correspond to results of the MCFM calculations. The bottom part of each subplot represents the ratio of the measured cross section to the expected one from POWHEG+GG2ZZ+PYTHIA (black crosses with solid symbols) and MCFM (red crosses). The shaded areas on all the plots represent the full uncertainties calculated as the quadrature sum of the statistical and systematic uncertainties, whereas the crosses represent the statistical uncertainties only. (For interpretation of the references to color in this figure legend, the reader is referred to the web version of this article.)

POWHEG and MCFM. The bottom part of each plot shows the ratio of the measured to the predicted values. The bin sizes were chosen according to the resolution of the relevant variables, trying also to keep the statistical uncertainties at a similar level for all the bins. Fig. 4 shows the angular correlations between Z bosons, which are in good agreement with the MC simulations. Some difference between POWHEG and MCFM calculations appears at very low p_T of the ZZ system and for azimuthal separation of the Z bosons close to π . This region is better modeled by POWHEG interfaced with the PYTHIA parton shower program.

8. Limits on anomalous triple gauge couplings

The presence of ATGCs would be manifested as an increased yield of events at high four-lepton masses. Fig. 5 presents the distribution of the four-lepton reconstructed mass, which is used to set the limits, for the combined 4e, 4 μ , and 2e2 μ channels. The shaded histogram represents the results of the POWHEG simulation

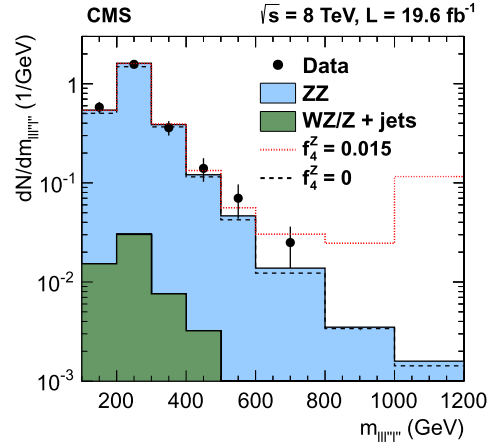


Fig. 5. Distribution of the four-lepton reconstructed mass for the combined 4e, 4 μ , and 2e2 μ channels. Points represent the data, the shaded histogram labeled ZZ represents the POWHEG+GG2ZZ+PYTHIA predictions for ZZ signal, the histograms labeled WZ/Z + jets shows background, which is estimated from data, as described in the text. The dashed and dotted histograms indicate the results of the SHERPA simulation for the SM ($f_4^Z = 0$) and in the presence of an ATGC ($f_4^Z = 0.015$) with all the other anomalous couplings set to zero. The last bin includes all entries with masses above 1000 GeV.

for the ZZ signal, and the dashed line, which agrees well with it, is the prediction of SHERPA for $f_4^Z = 0$ normalized to the MCFM cross section. The dotted line indicates the SHERPA predictions for a specific ATGC value ($f_4^Z = 0.015$) with all the other anomalous couplings set to zero.

The invariant mass distributions are interpolated from the SHERPA simulation for different values of the anomalous couplings in the range between 0 and 0.015. For each distribution, only one or two couplings are varied while all others are set to zero. The measured signal is obtained from a comparison of the data to a grid of ATGC models in the (f_4^Z, f_4^γ) and (f_5^Z, f_5^γ) parameter planes. Expected signal values are interpolated between the 2D grid points using a second-degree polynomial, since the cross section for signal depends quadratically on the coupling parameters. A profile likelihood method [33] is used to derive the limits. Systematic uncertainties are taken into account by varying the number of expected signal and background events within their uncertainties. No form factor is used when deriving the limits so that the results do not depend on any assumed energy scale characterizing new physics. The constraints on anomalous couplings are displayed in Fig. 6. The curves indicate 68% and 95% confidence levels, and the solid dot shows where the likelihood reaches its maximum. Coupling values outside the contours are excluded at the corresponding confidence levels. The limits are dominated by statistical uncertainties.

One-dimensional 95% CL limits for the $f_4^{Z,\gamma}$ and $f_5^{Z,\gamma}$ anomalous coupling parameters are:

$$\begin{aligned} -0.004 < f_4^Z < 0.004, \\ -0.004 < f_5^Z < 0.004, \\ -0.005 < f_4^\gamma < 0.005, \\ -0.005 < f_5^\gamma < 0.005. \end{aligned}$$

In the one-dimensional fits, all of the ATGC parameters except the one under study are set to zero. These values extend previous CMS results on vector boson self-interactions [3] and improve on the previous limits by factors of three to four, they are presented in Fig. 6 as horizontal and vertical lines.

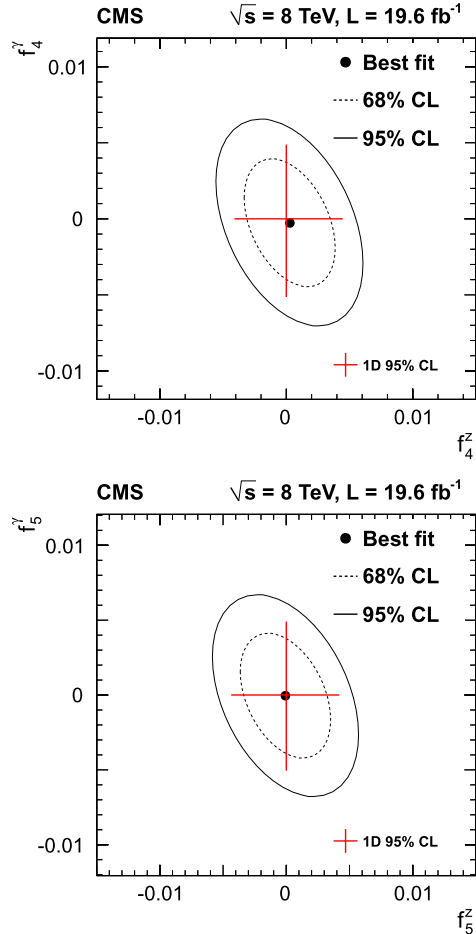


Fig. 6. Two-dimensional exclusion limits at 68% (dashed contour) and 95% (solid contour) CL on the ZZZ and ZZ γ ATGCs. The top (bottom) plot shows the exclusion contour in the ($f_{4(5)}^Z$, $f_{4(5)}^Y$) parameter planes. The solid dot shows where the likelihood reaches its maximum. The values of couplings outside of contours are excluded at the corresponding confidence level. The lines in the middle represent one-dimensional limits. No form factor is used.

9. Summary

Measurements have been presented of the inclusive ZZ production cross section in proton–proton collisions at 8 TeV in the ZZ $\rightarrow \ell\ell\ell'\ell'$ decay mode, with $\ell = e, \mu$ and $\ell' = e, \mu, \tau$. The data sample corresponds to an integrated luminosity of 19.6 fb^{-1} . The measured total cross section $\sigma(\text{pp} \rightarrow \text{ZZ}) = 7.7 \pm 0.5 \text{ (stat)}^{+0.5}_{-0.4} \text{ (syst)} \pm 0.4 \text{ (theo)} \pm 0.2 \text{ (lumi)} \text{ pb}$ for both Z bosons in the mass range $60 < m_Z < 120 \text{ GeV}$ and the differential cross sections agree well with the SM predictions. Improved limits on anomalous ZZZ and ZZ γ triple gauge couplings are established, significantly restricting their possible allowed ranges.

Acknowledgements

We congratulate our colleagues in the CERN accelerator departments for the excellent performance of the LHC and thank the technical and administrative staffs at CERN and at other CMS institutes for their contributions to the success of the CMS effort. In addition, we gratefully acknowledge the computing centres and personnel of the Worldwide LHC Computing Grid for delivering so effectively the computing infrastructure essential to our analyses. Finally, we acknowledge the enduring support for the construction and operation of the LHC and the CMS detector provided by the following funding agencies: BMWFW and FWF (Austria); FNRS

and FWO (Belgium); CNPq, CAPES, FAPERJ, and FAPESP (Brazil); MES (Bulgaria); CERN; CAS, MoST, and NSFC (China); COLCIENCIAS (Colombia); MSES and CSF (Croatia); RPF (Cyprus); MoER, ERC IUT and ERDF (Estonia); Academy of Finland, MEC, and HIP (Finland); CEA and CNRS/IN2P3 (France); BMBF, DFG, and HGF (Germany); GSRT (Greece); OTKA and NIH (Hungary); DAE and DST (India); IPM (Iran); SFI (Ireland); INFN (Italy); NRF and WCU (Republic of Korea); LAS (Lithuania); MOE and UM (Malaysia); CINVESTAV, CONACYT, SEP, and UASLP-FAI (Mexico); MBIE (New Zealand); PAEC (Pakistan); MSHE and NSC (Poland); FCT (Portugal); JINR (Dubna); MON, RosAtom, RAS and RFBR (Russia); MESTD (Serbia); SEIDI and CPAN (Spain); Swiss Funding Agencies (Switzerland); MST (Taipei); ThEPCenter, IPST, STAR and NSTDA (Thailand); TUBITAK and TAEK (Turkey); NASU and SFFR (Ukraine); STFC (United Kingdom); DOE and NSF (USA).

Individuals have received support from the Marie-Curie programme and the European Research Council and EPLANET (European Union); the Leventis Foundation; the A.P. Sloan Foundation; the Alexander von Humboldt Foundation; the Belgian Federal Science Policy Office; the Fonds pour la Formation à la Recherche dans l’Industrie et dans l’Agriculture (FRIA-Belgium); the Agentschap voor Innovatie door Wetenschap en Technologie (IWT-Belgium); the Ministry of Education, Youth and Sports (MEYS) of the Czech Republic; the Council of Science and Industrial Research, India; the HOMING PLUS programme of Foundation For Polish Science, cofinanced from European Union, Regional Development Fund; the Compagnia di San Paolo (Torino); and the Thalis and Aristeia programmes cofinanced by EU-ESF and the Greek NSRF.

References

- [1] K. Hagiwara, R.D. Peccei, D. Zeppenfeld, Probing the weak boson sector in $e^+e^- \rightarrow W^+W^-$, Nucl. Phys. B 282 (1987) 253, [http://dx.doi.org/10.1016/0550-3213\(87\)90685-7](http://dx.doi.org/10.1016/0550-3213(87)90685-7).
- [2] G.J. Gounaris, J. Layssac, F.M. Renard, New and standard physics contributions to anomalous Z and gamma self-couplings, Phys. Rev. D 62 (2000) 073013, <http://dx.doi.org/10.1103/PhysRevD.62.073013>, arXiv:hep-ph/0003143.
- [3] CMS Collaboration, Measurement of the ZZ production cross section and search for anomalous couplings in $2\ell 2\ell'$ final states in pp collisions at $\sqrt{s} = 7 \text{ TeV}$, J. High Energy Phys. 01 (2013) 063, [http://dx.doi.org/10.1007/JHEP01\(2013\)063](http://dx.doi.org/10.1007/JHEP01(2013)063), arXiv:1211.4890.
- [4] CMS Collaboration, Measurement of W^+W^- and ZZ production cross sections in pp collisions at $\sqrt{s} = 8 \text{ TeV}$, Phys. Lett. B 721 (2013) 190, <http://dx.doi.org/10.1016/j.physletb.2013.03.027>, arXiv:1301.4698.
- [5] ATLAS Collaboration, Measurement of ZZ production in pp collisions at $\sqrt{s} = 7 \text{ TeV}$ and limits on anomalous ZZZ and ZZ γ couplings with the ATLAS detector, J. High Energy Phys. 03 (2013) 128, [http://dx.doi.org/10.1007/JHEP03\(2013\)128](http://dx.doi.org/10.1007/JHEP03(2013)128), arXiv:1211.6096.
- [6] T. Aaltonen, et al., CDF Collaboration, Measurement of ZZ production in leptonic final states at \sqrt{s} of 1.96 TeV at CDF, Phys. Rev. Lett. 108 (2012) 101801, <http://dx.doi.org/10.1103/PhysRevLett.108.101801>, arXiv:1112.2978.
- [7] V.M. Abazov, et al., D0 Collaboration, Measurement of the ZZ production cross section in $p\bar{p}$ collisions at $\sqrt{s} = 1.96 \text{ TeV}$, Phys. Rev. D 84 (2011) 011103, <http://dx.doi.org/10.1103/PhysRevD.84.011103>, arXiv:1104.3078.
- [8] CMS Collaboration, The CMS experiment at the CERN LHC, J. Instrum. 3 (2008) 08004, <http://dx.doi.org/10.1088/1748-0221/3/08/S08004>.
- [9] S. Alioli, P. Nason, C. Oleari, E. Re, NLO vector-boson production matched with shower in POWHEG, J. High Energy Phys. 07 (2008) 060, <http://dx.doi.org/10.1088/1126-6708/2008/07/060>, arXiv:0805.4802.
- [10] P. Nason, A new method for combining NLO QCD with shower Monte Carlo algorithms, J. High Energy Phys. 11 (2004) 040, <http://dx.doi.org/10.1088/1126-6708/2004/11/040>, arXiv:hep-ph/0409146.
- [11] S. Frixione, P. Nason, C. Oleari, Matching NLO QCD computations with parton shower simulations: the POWHEG method, J. High Energy Phys. 11 (2007) 070, <http://dx.doi.org/10.1088/1126-6708/2007/11/070>, arXiv:0709.2092.
- [12] T. Gleisberg, S. Höche, F. Krauss, M. Schönherr, S. Schumann, F. Siegert, J. Winter, Event generation with SHERPA 1.1, J. High Energy Phys. 02 (2009) 007, <http://dx.doi.org/10.1088/1126-6708/2009/02/007>, arXiv:0811.4622.
- [13] T. Binoth, N. Kauer, P. Mertsch, Gluon-induced QCD corrections to $\text{pp} \rightarrow ZZ \rightarrow \ell\ell\ell'\ell'$, <http://dx.doi.org/10.3360/diss.2008.142>, arXiv:0807.0024, 2008.
- [14] J. Alwall, M. Herquet, F. Maltoni, O. Mattelaer, T. Stelzer, Madgraph 5: going beyond, J. High Energy Phys. 06 (2011) 128, [http://dx.doi.org/10.1007/JHEP06\(2011\)128](http://dx.doi.org/10.1007/JHEP06(2011)128), arXiv:1106.0522.

- [15] T. Sjöstrand, S. Mrenna, P.Z. Skands, PYTHIA 6.4 physics and manual, J. High Energy Phys. 05 (2006) 026, <http://dx.doi.org/10.1088/1126-6708/2006/05/026>, arXiv:hep-ph/0603175.
- [16] H.-L. Lai, J. Huston, Z. Li, P. Nadolsky, J. Pumplin, D. Stump, C.-P. Yuan, Uncertainty induced by QCD coupling in the CTEQ global analysis of parton distributions, Phys. Rev. D 82 (2010) 054021, <http://dx.doi.org/10.1103/PhysRevD.82.054021>, arXiv:1004.4624.
- [17] H.-L. Lai, M. Guzzi, J. Huston, Z. Li, P. Nadolsky, J. Pumplin, C.-P. Yuan, New parton distributions for collider physics, Phys. Rev. D 82 (2010) 074024, <http://dx.doi.org/10.1103/PhysRevD.82.074024>, arXiv:1007.2241.
- [18] J.M. Campbell, R.K. Ellis, MCFM for the Tevatron and the LHC, Nucl. Phys. B, Proc. Suppl. 205 (2010) 10, <http://dx.doi.org/10.1016/j.nuclphysbps.2010.08.011>, arXiv:1007.3492.
- [19] A.D. Martin, W.J. Stirling, R.S. Thorne, G. Watt, Parton distributions for the LHC, Eur. Phys. J. C 63 (2009) 189, <http://dx.doi.org/10.1140/epjc/s10052-009-1072-5>, arXiv:0901.0002.
- [20] S. Jadach, Z. Wąs, The tau decay library TAUOLA: version 2.4, Comput. Phys. Commun. 76 (1993) 361, [http://dx.doi.org/10.1016/0010-4655\(93\)90061-G](http://dx.doi.org/10.1016/0010-4655(93)90061-G).
- [21] S. Agostinelli, et al., GEANT4 Collaboration, Geant4—a simulation toolkit, Nucl. Instrum. Methods, Sect. A 506 (2003) 250, [http://dx.doi.org/10.1016/S0168-9002\(03\)01368-8](http://dx.doi.org/10.1016/S0168-9002(03)01368-8).
- [22] CMS Collaboration, Particle-flow event reconstruction in CMS and performance for Jets, Taus, and E_T^{miss} , CMS Physics Analysis Summary CMS-PAS-PFT-09-001, <http://cdsweb.cern.ch/record/1194487>, 2009.
- [23] CMS Collaboration, Commissioning of the Particle-flow Event Reconstruction with the first LHC collisions recorded in the CMS detector, CMS Physics Analysis Summary CMS-PAS-PFT-10-001, <http://cdsweb.cern.ch/record/1247373>, 2010.
- [24] S. Baffioni, C. Charlot, F. Ferri, D. Futyan, P. Meridiani, I. Puljak, C. Rovelli, R. Salerno, Y. Sirois, Electron reconstruction in CMS, Eur. Phys. J. C 49 (2007) 1099, <http://dx.doi.org/10.1140/epjc/s10052-006-0175-5>.
- [25] W. Adam, R. Fröhlich, A. Strandlie, T. Todorov, Reconstruction of electrons with the Gaussian-sum filter in the CMS tracker at the LHC, J. Phys. G, Nucl. Part. Phys. 31 (2005) N9, <http://dx.doi.org/10.1088/0954-3899/31/9/N01>.
- [26] CMS Collaboration, Performance of CMS muon reconstruction in pp collision events at $\sqrt{s} = 7$ TeV, J. Instrum. 7 (2012) P10002, <http://dx.doi.org/10.1088/1748-0221/7/10/P10002>, arXiv:1206.4071.
- [27] CMS Collaboration, Performance of τ -lepton reconstruction and identification in CMS, J. Instrum. 7 (2012) P01001, <http://dx.doi.org/10.1088/1748-0221/7/01/P01001>.
- [28] M. Cacciari, G.P. Salam, Pileup subtraction using jet areas, Phys. Lett. B 659 (2008) 119, <http://dx.doi.org/10.1016/j.physletb.2007.09.077>, arXiv:0707.1378.
- [29] CMS Collaboration, Measurement of the inclusive W and Z production cross sections in pp collisions at $\sqrt{s} = 7$ TeV, J. High Energy Phys. 10 (2011) 132, [http://dx.doi.org/10.1007/JHEP10\(2011\)132](http://dx.doi.org/10.1007/JHEP10(2011)132), arXiv:1107.4789.
- [30] CMS Collaboration, CMS luminosity based on pixel cluster counting – Summer 2013 update, CMS Physics Analysis Summary CMS-PAS-LUM-13-001, <https://cds.cern.ch/record/1598864>, 2013.
- [31] M. Botje, J. Butterworth, A. Cooper-Sarkar, A. de Roeck, J. Feltesse, S. Forte, A. Glazov, J. Huston, R. McNulty, T. Sjöstrand, R. Thorne, The PDF4LHC working group interim recommendations, arXiv:1101.0538, 2011.
- [32] D.R. Ball, V. Bertone, F. Cerutti, L. Del Debbio, S. Forte, A. Guffanti, J.I. Latorre, J. Rojo, M. Ubiali, Impact of heavy quark masses on parton distributions and lhc phenomenology, Nucl. Phys. B 849 (2011) 296, <http://dx.doi.org/10.1016/j.nuclphysb.2011.03.021>, arXiv:1101.1300.
- [33] J. Beringer, et al., Particle Data Group, Review of particle physics, Phys. Rev. D 86 (2012) 010001, <http://dx.doi.org/10.1103/PhysRevD.86.010001>.
- [34] G. D'Agostini, Improved iterative Bayesian unfolding, arXiv:1010.0632, 2010.

CMS Collaboration

V. Khachatryan, A.M. Sirunyan, A. Tumasyan

Yerevan Physics Institute, Yerevan, Armenia

W. Adam, T. Bergauer, M. Dragicevic, J. Erö, C. Fabjan¹, M. Friedl, R. Fröhlich¹, V.M. Ghete, C. Hartl, N. Hörmann, J. Hrubec, M. Jeitler¹, W. Kiesenhofer, V. Knünz, M. Krammer¹, I. Krätschmer, D. Liko, I. Mikulec, D. Rabady², B. Rahbaran, H. Rohringer, R. Schöfbeck, J. Strauss, A. Taurok, W. Treberer-Treberspurg, W. Waltenberger, C.-E. Wulz¹

Institut für Hochenergiephysik der OeAW, Wien, Austria

V. Mossolov, N. Shumeiko, J. Suarez Gonzalez

National Centre for Particle and High Energy Physics, Minsk, Belarus

S. Alderweireldt, M. Bansal, S. Bansal, T. Cornelis, E.A. De Wolf, X. Janssen, A. Knutsson, S. Luyckx, S. Ochesanu, B. Roland, R. Rougny, M. Van De Klundert, H. Van Haevermaet, P. Van Mechelen, N. Van Remortel, A. Van Spilbeeck

Universiteit Antwerpen, Antwerpen, Belgium

F. Blekman, S. Blyweert, J. D'Hondt, N. Daci, N. Heracleous, A. Kalogeropoulos, J. Keaveney, T.J. Kim, S. Lowette, M. Maes, A. Olbrechts, Q. Python, D. Strom, S. Tavernier, W. Van Doninck, P. Van Mulders, G.P. Van Onsem, I. Villegas

Vrije Universiteit Brussel, Brussel, Belgium

C. Caillol, B. Clerbaux, G. De Lentdecker, D. Dobur, L. Favart, A.P.R. Gay, A. Grebenyuk, A. Léonard, A. Mohammadi, L. Perniè², T. Reis, T. Seva, L. Thomas, C. Vander Velde, P. Vanlaer, J. Wang

Université Libre de Bruxelles, Bruxelles, Belgium

V. Adler, K. Beernaert, L. Benucci, A. Cimmino, S. Costantini, S. Crucy, S. Dildick, A. Fagot, G. Garcia, B. Klein, J. Mccartin, A.A. Ocampo Rios, D. Ryckbosch, S. Salva Diblen, M. Sigamani, N. Strobbe,

F. Thyssen, M. Tytgat, E. Yazgan, N. Zaganidis

Ghent University, Ghent, Belgium

S. Basegmez, C. Beluffi³, G. Bruno, R. Castello, A. Caudron, L. Ceard, G.G. Da Silveira, C. Delaere, T. du Pree, D. Favart, L. Forthomme, A. Giannanco⁴, J. Hollar, P. Jez, M. Komm, V. Lemaitre, J. Liao, C. Nuttens, D. Pagano, A. Pin, K. Piotrzkowski, A. Popov⁵, L. Quertenmont, M. Selvaggi, M. Vidal Marono, J.M. Vizan Garcia

Université Catholique de Louvain, Louvain-la-Neuve, Belgium

N. Belyi, T. Caebergs, E. Daubie, G.H. Hammad

Université de Mons, Mons, Belgium

G.A. Alves, M. Correa Martins Junior, T. Dos Reis Martins, M.E. Pol

Centro Brasileiro de Pesquisas Fisicas, Rio de Janeiro, Brazil

W.L. Aldá Júnior, W. Carvalho, J. Chinellato⁶, A. Custódio, E.M. Da Costa, D. De Jesus Damiao, C. De Oliveira Martins, S. Fonseca De Souza, H. Malbouisson, M. Malek, D. Matos Figueiredo, L. Mundim, H. Nogima, W.L. Prado Da Silva, J. Santaolalla, A. Santoro, A. Sznajder, E.J. Tonelli Manganote⁶, A. Vilela Pereira

Universidade do Estado do Rio de Janeiro, Rio de Janeiro, Brazil

C.A. Bernardes^b, F.A. Dias^{a,7}, T.R. Fernandez Perez Tomei^a, E.M. Gregores^b, P.G. Mercadante^b, S.F. Novaes^a, Sandra S. Padula^a

^a *Universidade Estadual Paulista, São Paulo, Brazil*

^b *Universidade Federal do ABC, São Paulo, Brazil*

A. Aleksandrov, V. Genchev², P. Iaydjiev, A. Marinov, S. Piperov, M. Rodozov, G. Sultanov, M. Vutova

Institute for Nuclear Research and Nuclear Energy, Sofia, Bulgaria

A. Dimitrov, I. Glushkov, R. Hadjiiska, V. Kozuharov, L. Litov, B. Pavlov, P. Petkov

University of Sofia, Sofia, Bulgaria

J.G. Bian, G.M. Chen, H.S. Chen, M. Chen, R. Du, C.H. Jiang, D. Liang, S. Liang, R. Plestina⁸, J. Tao, X. Wang, Z. Wang

Institute of High Energy Physics, Beijing, China

C. Asawatangtrakuldee, Y. Ban, Y. Guo, Q. Li, W. Li, S. Liu, Y. Mao, S.J. Qian, D. Wang, L. Zhang, W. Zou

State Key Laboratory of Nuclear Physics and Technology, Peking University, Beijing, China

C. Avila, L.F. Chaparro Sierra, C. Florez, J.P. Gomez, B. Gomez Moreno, J.C. Sanabria

Universidad de Los Andes, Bogota, Colombia

N. Godinovic, D. Lelas, D. Polic, I. Puljak

Technical University of Split, Split, Croatia

Z. Antunovic, M. Kovac

University of Split, Split, Croatia

V. Brigljevic, K. Kadija, J. Luetic, D. Mekterovic, L. Sudic

Institute Rudjer Boskovic, Zagreb, Croatia

A. Attikis, G. Mavromanolakis, J. Mousa, C. Nicolaou, F. Ptochos, P.A. Razis

University of Cyprus, Nicosia, Cyprus

M. Bodlak, M. Finger, M. Finger Jr.

Charles University, Prague, Czech Republic

Y. Assran⁹, A. Ellithi Kamel¹⁰, M.A. Mahmoud¹¹, A. Radi^{12,13}

Academy of Scientific Research and Technology of the Arab Republic of Egypt, Egyptian Network of High Energy Physics, Cairo, Egypt

M. Kadastik, M. Murumaa, M. Raidal, A. Tiko

National Institute of Chemical Physics and Biophysics, Tallinn, Estonia

P. Eerola, G. Fedi, M. Voutilainen

Department of Physics, University of Helsinki, Helsinki, Finland

J. Häkkinen, V. Karimäki, R. Kinnunen, M.J. Kortelainen, T. Lampén, K. Lassila-Perini, S. Lehti, T. Lindén, P. Luukka, T. Mäenpää, T. Peltola, E. Tuominen, J. Tuominiemi, E. Tuovinen, L. Wendland

Helsinki Institute of Physics, Helsinki, Finland

T. Tuuva

Lappeenranta University of Technology, Lappeenranta, Finland

M. Besancon, F. Couderc, M. Dejardin, D. Denegri, B. Fabbro, J.L. Faure, C. Favaro, F. Ferri, S. Ganjour, A. Givernaud, P. Gras, G. Hamel de Monchenault, P. Jarry, E. Locci, J. Malcles, A. Nayak, J. Rander, A. Rosowsky, M. Titov

DSM/IRFU, CEA/Saclay, Gif-sur-Yvette, France

S. Baffioni, F. Beaudette, P. Busson, C. Charlot, T. Dahms, M. Dalchenko, L. Dobrzynski, N. Filipovic, A. Florent, R. Granier de Cassagnac, L. Mastrolorenzo, P. Miné, C. Mironov, I.N. Naranjo, M. Nguyen, C. Ochando, P. Paganini, R. Salerno, J.B. Sauvan, Y. Sirois, C. Veelken, Y. Yilmaz, A. Zabi

Laboratoire Leprince-Ringuet, Ecole Polytechnique, IN2P3-CNRS, Palaiseau, France

J.-L. Agram¹⁴, J. Andrea, A. Aubin, D. Bloch, J.-M. Brom, E.C. Chabert, C. Collard, E. Conte¹⁴, J.-C. Fontaine¹⁴, D. Gelé, U. Goerlach, C. Goetzmann, A.-C. Le Bihan, P. Van Hove

Institut Pluridisciplinaire Hubert Curien, Université de Strasbourg, Université de Haute Alsace Mulhouse, CNRS/IN2P3, Strasbourg, France

S. Gadrat

Centre de Calcul de l'Institut National de Physique Nucléaire et de Physique des Particules, CNRS/IN2P3, Villeurbanne, France

S. Beauceron, N. Beaupere, G. Boudoul², S. Brochet, C.A. Carrillo Montoya, J. Chasserat, R. Chierici, D. Contardo², P. Depasse, H. El Mamouni, J. Fan, J. Fay, S. Gascon, M. Gouzevitch, B. Ille, T. Kurca, M. Lethuillier, L. Mirabito, S. Perries, J.D. Ruiz Alvarez, D. Sabes, L. Sgandurra, V. Sordini, M. Vander Donckt, P. Verdier, S. Viret, H. Xiao

Université de Lyon, Université Claude Bernard Lyon 1, CNRS-IN2P3, Institut de Physique Nucléaire de Lyon, Villeurbanne, France

Z. Tsamalaidze¹⁵

Institute of High Energy Physics and Informatization, Tbilisi State University, Tbilisi, Georgia

C. Autermann, S. Beranek, M. Bontenackels, B. Calpas, M. Edelhoff, L. Feld, O. Hindrichs, K. Klein, A. Ostapchuk, A. Perieanu, F. Raupach, J. Sammet, S. Schael, D. Sprenger, H. Weber,

B. Wittmer, V. Zhukov⁵

RWTH Aachen University, I. Physikalisches Institut, Aachen, Germany

M. Ata, J. Caudron, E. Dietz-Laursonn, D. Duchardt, M. Erdmann, R. Fischer, A. Güth, T. Hebbeker, C. Heidemann, K. Hoepfner, D. Klingebiel, S. Knutzen, P. Kreuzer, M. Merschmeyer, A. Meyer, M. Olszewski, K. Padeken, P. Papacz, H. Reithler, S.A. Schmitz, L. Sonnenschein, D. Teyssier, S. Thüer, M. Weber

RWTH Aachen University, III. Physikalisches Institut A, Aachen, Germany

V. Cherepanov, Y. Erdogan, G. Flügge, H. Geenen, M. Geisler, W. Haj Ahmad, F. Hoehle, B. Kargoll, T. Kress, Y. Kuessel, J. Lingemann², A. Nowack, I.M. Nugent, L. Perchalla, O. Pooth, A. Stahl

RWTH Aachen University, III. Physikalisches Institut B, Aachen, Germany

I. Asin, N. Bartosik, J. Behr, W. Behrenhoff, U. Behrens, A.J. Bell, M. Bergholz¹⁶, A. Bethani, K. Borras, A. Burgmeier, A. Cakir, L. Calligaris, A. Campbell, S. Choudhury, F. Costanza, C. Diez Pardos, S. Dooling, T. Dorland, G. Eckerlin, D. Eckstein, T. Eichhorn, G. Flucke, J. Garay Garcia, A. Geiser, P. Gunnellini, J. Hauk, G. Hellwig, M. Hempel, D. Horton, H. Jung, M. Kasemann, P. Katsas, J. Kieseler, C. Kleinwort, D. Krücker, W. Lange, J. Leonard, K. Lipka, A. Lobanov, W. Lohmann¹⁶, B. Lutz, R. Mankel, I. Marfin, I.-A. Melzer-Pellmann, A.B. Meyer, J. Mnich, A. Mussgiller, S. Naumann-Emme, O. Novgorodova, F. Nowak, E. Ntomari, H. Perrey, D. Pitzl, R. Placakyte, A. Raspereza, P.M. Ribeiro Cipriano, E. Ron, M.Ö. Sahin, J. Salfeld-Nebgen, P. Saxena, R. Schmidt¹⁶, T. Schoerner-Sadenius, M. Schröder, S. Spannagel, A.D.R. Vargas Trevino, R. Walsh, C. Wissing

Deutsches Elektronen-Synchrotron, Hamburg, Germany

M. Aldaya Martin, V. Blobel, M. Centis Vignali, J. Erfle, E. Garutti, K. Goebel, M. Görner, M. Gosselink, J. Haller, R.S. Höing, H. Kirschenmann, R. Klanner, R. Kogler, J. Lange, T. Lapsien, T. Lenz, I. Marchesini, J. Ott, T. Peiffer, N. Pietsch, D. Rathjens, C. Sander, H. Schettler, P. Schleper, E. Schlieckau, A. Schmidt, M. Seidel, J. Sibille¹⁷, V. Sola, H. Stadie, G. Steinbrück, D. Troendle, E. Usai, L. Vanelderden

University of Hamburg, Hamburg, Germany

C. Barth, C. Baus, J. Berger, C. Böser, E. Butz, T. Chwalek, W. De Boer, A. Descroix, A. Dierlamm, M. Feindt, F. Hartmann², T. Hauth², U. Husemann, I. Katkov⁵, A. Kornmayer², E. Kuznetsova, P. Lobelle Pardo, M.U. Mozer, Th. Müller, A. Nürnberg, G. Quast, K. Rabbertz, F. Ratnikov, S. Röcker, H.J. Simonis, F.M. Stober, R. Ulrich, J. Wagner-Kuhr, S. Wayand, T. Weiler, R. Wolf

Institut für Experimentelle Kernphysik, Karlsruhe, Germany

G. Anagnostou, G. Daskalakis, T. Geralis, V.A. Giakoumopoulou, A. Kyriakis, D. Loukas, A. Markou, C. Markou, A. Psallidas, I. Topsis-Giotis

Institute of Nuclear and Particle Physics (INPP), NCSR Demokritos, Aghia Paraskevi, Greece

L. Gouskos, A. Panagiotou, N. Saoulidou, E. Stiliaris

University of Athens, Athens, Greece

X. Aslanoglou, I. Evangelou, G. Flouris, C. Foudas, P. Kokkas, N. Manthos, I. Papadopoulos, E. Paradas

University of Ioánnina, Ioánnina, Greece

G. Bencze, C. Hajdu, P. Hidas, D. Horvath¹⁸, F. Sikler, V. Veszpremi, G. Vesztergombi¹⁹, A.J. Zsigmond

Wigner Research Centre for Physics, Budapest, Hungary

N. Beni, S. Czellar, J. Karancsi²⁰, J. Molnar, J. Palinkas, Z. Szillasi

Institute of Nuclear Research ATOMKI, Debrecen, Hungary

P. Raics, Z.L. Trocsanyi, B. Ujvari

University of Debrecen, Debrecen, Hungary

S.K. Swain

National Institute of Science Education and Research, Bhubaneswar, India

S.B. Beri, V. Bhatnagar, N. Dhingra, R. Gupta, A.K. Kalsi, M. Kaur, M. Mittal, N. Nishu, J.B. Singh

Panjab University, Chandigarh, India

Ashok Kumar, Arun Kumar, S. Ahuja, A. Bhardwaj, B.C. Choudhary, A. Kumar, S. Malhotra, M. Naimuddin, K. Ranjan, V. Sharma

University of Delhi, Delhi, India

S. Banerjee, S. Bhattacharya, K. Chatterjee, S. Dutta, B. Gomber, Sa. Jain, Sh. Jain, R. Khurana, A. Modak, S. Mukherjee, D. Roy, S. Sarkar, M. Sharan

Saha Institute of Nuclear Physics, Kolkata, India

A. Abdulsalam, D. Dutta, S. Kailas, V. Kumar, A.K. Mohanty², L.M. Pant, P. Shukla, A. Topkar

Bhabha Atomic Research Centre, Mumbai, India

T. Aziz, S. Banerjee, R.M. Chatterjee, R.K. Dewanjee, S. Dugad, S. Ganguly, S. Ghosh, M. Guchait, A. Gurto²¹, G. Kole, S. Kumar, M. Maity²², G. Majumder, K. Mazumdar, G.B. Mohanty, B. Parida, K. Sudhakar, N. Wickramage²³

Tata Institute of Fundamental Research, Mumbai, India

H. Bakhshiansohi, H. Behnamian, S.M. Etesami²⁴, A. Fahim²⁵, R. Goldouzian, A. Jafari, M. Khakzad, M. Mohammadi Najafabadi, M. Naseri, S. Pakhtinat Mehdiabadi, B. Safarzadeh²⁶, M. Zeinali

Institute for Research in Fundamental Sciences (IPM), Tehran, Iran

M. Felcini, M. Grunewald

University College Dublin, Dublin, Ireland

M. Abbrescia^{a,b}, L. Barbone^{a,b}, C. Calabria^{a,b}, S.S. Chhibra^{a,b}, A. Colaleo^a, D. Creanza^{a,c}, N. De Filippis^{a,c}, M. De Palma^{a,b}, L. Fiore^a, G. Iaselli^{a,c}, G. Maggi^{a,c}, M. Maggi^a, S. My^{a,c}, S. Nuzzo^{a,b}, N. Pacifico^a, A. Pompili^{a,b}, G. Pugliese^{a,c}, R. Radogna^{a,b,2}, G. Selvaggi^{a,b}, L. Silvestris^{a,2}, G. Singh^{a,b}, R. Venditti^{a,b}, P. Verwilligen^a, G. Zito^a

^a INFN Sezione di Bari, Bari, Italy

^b Università di Bari, Bari, Italy

^c Politecnico di Bari, Bari, Italy

G. Abbiendi^a, A.C. Benvenuti^a, D. Bonacorsi^{a,b}, S. Braibant-Giacomelli^{a,b}, L. Brigliadori^{a,b}, R. Campanini^{a,b}, P. Capiluppi^{a,b}, A. Castro^{a,b}, F.R. Cavallo^a, G. Codispoti^{a,b}, M. Cuffiani^{a,b}, G.M. Dallavalle^a, F. Fabbri^a, A. Fanfani^{a,b}, D. Fasanella^{a,b}, P. Giacomelli^a, C. Grandi^a, L. Guiducci^{a,b}, S. Marcellini^a, G. Masetti^{a,2}, A. Montanari^a, F.L. Navarria^{a,b}, A. Perrotta^a, F. Primavera^{a,b}, A.M. Rossi^{a,b}, T. Rovelli^{a,b}, G.P. Siroli^{a,b}, N. Tosi^{a,b}, R. Travaglini^{a,b}

^a INFN Sezione di Bologna, Bologna, Italy

^b Università di Bologna, Bologna, Italy

S. Albergo^{a,b}, G. Cappello^a, M. Chiorboli^{a,b}, S. Costa^{a,b}, F. Giordano^{a,2}, R. Potenza^{a,b}, A. Tricomi^{a,b}, C. Tuve^{a,b}

^a INFN Sezione di Catania, Catania, Italy

^b Università di Catania, Catania, Italy

^c CSFNSM, Catania, Italy

G. Barbagli ^a, V. Ciulli ^{a,b}, C. Civinini ^a, R. D'Alessandro ^{a,b}, E. Focardi ^{a,b}, E. Gallo ^a, S. Gonzi ^{a,b}, V. Gori ^{a,b,2}, P. Lenzi ^{a,b}, M. Meschini ^a, S. Paoletti ^a, G. Sguazzoni ^a, A. Tropiano ^{a,b}

^a INFN Sezione di Firenze, Firenze, Italy
^b Università di Firenze, Firenze, Italy

L. Benussi, S. Bianco, F. Fabbri, D. Piccolo

INFN Laboratori Nazionali di Frascati, Frascati, Italy

F. Ferro ^a, M. Lo Vetere ^{a,b}, E. Robutti ^a, S. Tosi ^{a,b}

^a INFN Sezione di Genova, Genova, Italy
^b Università di Genova, Genova, Italy

M.E. Dinardo ^{a,b}, S. Fiorendi ^{a,b,2}, S. Gennai ^{a,2}, R. Gerosa ², A. Ghezzi ^{a,b}, P. Govoni ^{a,b}, M.T. Lucchini ^{a,b,2}, S. Malvezzi ^a, R.A. Manzoni ^{a,b}, A. Martelli ^{a,b}, B. Marzocchi, D. Menasce ^a, L. Moroni ^a, M. Paganoni ^{a,b}, D. Pedrini ^a, S. Ragazzi ^{a,b}, N. Redaelli ^a, T. Tabarelli de Fatis ^{a,b}

^a INFN Sezione di Milano-Bicocca, Milano, Italy
^b Università di Milano-Bicocca, Milano, Italy

S. Buontempo ^a, N. Cavallo ^{a,c}, S. Di Guida ^{a,d,2}, F. Fabozzi ^{a,c}, A.O.M. Iorio ^{a,b}, L. Lista ^a, S. Meola ^{a,d,2}, M. Merola ^a, P. Paolucci ^{a,2}

^a INFN Sezione di Napoli, Napoli, Italy
^b Università di Napoli 'Federico II', Napoli, Italy
^c Università della Basilicata (Potenza), Napoli, Italy
^d Università G. Marconi (Roma), Napoli, Italy

P. Azzi ^a, N. Bacchetta ^a, D. Bisello ^{a,b}, A. Branca ^{a,b}, R. Carlin ^{a,b}, P. Checchia ^a, M. Dall'Osso ^{a,b}, T. Dorigo ^a, U. Dosselli ^a, M. Galanti ^{a,b}, F. Gasparini ^{a,b}, U. Gasparini ^{a,b}, P. Giubilato ^{a,b}, A. Gozzelino ^a, K. Kanishchev ^{a,c}, S. Lacaprara ^a, M. Margoni ^{a,b}, J. Pazzini ^{a,b}, M. Pegoraro ^a, N. Pozzobon ^{a,b}, P. Ronchese ^{a,b}, F. Simonetto ^{a,b}, M. Tosi ^{a,b}, A. Triassi ^a, S. Ventura ^a, A. Zucchetta ^{a,b}, G. Zumerle ^{a,b}

^a INFN Sezione di Padova, Padova, Italy
^b Università di Padova, Padova, Italy
^c Università di Trento (Trento), Padova, Italy

M. Gabusi ^{a,b}, S.P. Ratti ^{a,b}, C. Riccardi ^{a,b}, P. Salvini ^a, P. Vitulo ^{a,b}

^a INFN Sezione di Pavia, Pavia, Italy
^b Università di Pavia, Pavia, Italy

M. Biasini ^{a,b}, G.M. Bilei ^a, D. Ciangottini ^{a,b}, L. Fanò ^{a,b}, P. Lariccia ^{a,b}, G. Mantovani ^{a,b}, M. Menichelli ^a, F. Romeo ^{a,b}, A. Saha ^a, A. Santocchia ^{a,b}, A. Spiezia ^{a,b,2}

^a INFN Sezione di Perugia, Perugia, Italy
^b Università di Perugia, Perugia, Italy

K. Androsov ^{a,27}, P. Azzurri ^a, G. Bagliesi ^a, J. Bernardini ^a, T. Boccali ^a, G. Broccolo ^{a,c}, R. Castaldi ^a, M.A. Ciocci ^{a,27}, R. Dell'Orso ^a, S. Donato ^{a,c}, F. Fiori ^{a,c}, L. Foà ^{a,c}, A. Giassi ^a, M.T. Grippo ^{a,27}, F. Ligabue ^{a,c}, T. Lomtadze ^a, L. Martini ^{a,b}, A. Messineo ^{a,b}, C.S. Moon ^{a,28}, F. Palla ^{a,2}, A. Rizzi ^{a,b}, A. Savoy-Navarro ^{a,29}, A.T. Serban ^a, P. Spagnolo ^a, P. Squillaciotti ^{a,27}, R. Tenchini ^a, G. Tonelli ^{a,b}, A. Venturi ^a, P.G. Verdini ^a, C. Vernieri ^{a,c,2}

^a INFN Sezione di Pisa, Pisa, Italy
^b Università di Pisa, Pisa, Italy
^c Scuola Normale Superiore di Pisa, Pisa, Italy

L. Barone ^{a,b}, F. Cavallari ^a, D. Del Re ^{a,b}, M. Diemoz ^a, M. Grassi ^{a,b}, C. Jorda ^a, E. Longo ^{a,b}, F. Margaroli ^{a,b}, P. Meridiani ^a, F. Micheli ^{a,b,2}, S. Nourbakhsh ^{a,b}, G. Organtini ^{a,b}, R. Paramatti ^a, S. Rahatlou ^{a,b}, C. Rovelli ^a, F. Santanastasio ^{a,b}, L. Soffi ^{a,b,2}, P. Traczyk ^{a,b}

^a INFN Sezione di Roma, Roma, Italy
^b Università di Roma, Roma, Italy

N. Amapane ^{a,b}, R. Arcidiacono ^{a,c}, S. Argiro ^{a,b,2}, M. Arneodo ^{a,c}, R. Bellan ^{a,b}, C. Biino ^a, N. Cartiglia ^a, S. Casasso ^{a,b,2}, M. Costa ^{a,b}, A. Degano ^{a,b}, N. Demaria ^a, L. Finco ^{a,b}, C. Mariotti ^a, S. Maselli ^a, E. Migliore ^{a,b}, V. Monaco ^{a,b}, M. Musich ^a, M.M. Obertino ^{a,c,2}, G. Ortona ^{a,b}, L. Pacher ^{a,b}, N. Pastrone ^a, M. Pelliccioni ^a, G.L. Pinna Angioni ^{a,b}, A. Potenza ^{a,b}, A. Romero ^{a,b}, M. Ruspa ^{a,c}, R. Sacchi ^{a,b}, A. Solano ^{a,b}, A. Staiano ^a, U. Tamponi ^a

^a INFN Sezione di Torino, Torino, Italy

^b Università di Torino, Torino, Italy

^c Università del Piemonte Orientale (Novara), Torino, Italy

S. Belforte ^a, V. Candelise ^{a,b}, M. Casarsa ^a, F. Cossutti ^a, G. Della Ricca ^{a,b}, B. Gobbo ^a, C. La Licata ^{a,b}, M. Marone ^{a,b}, D. Montanino ^{a,b}, A. Schizzi ^{a,b,2}, T. Umer ^{a,b}, A. Zanetti ^a

^a INFN Sezione di Trieste, Trieste, Italy

^b Università di Trieste, Trieste, Italy

S. Chang, A. Kropivnitskaya, S.K. Nam

Kangwon National University, Chunchon, Republic of Korea

D.H. Kim, G.N. Kim, M.S. Kim, D.J. Kong, S. Lee, Y.D. Oh, H. Park, A. Sakharov, D.C. Son

Kyungpook National University, Daegu, Republic of Korea

J.Y. Kim, S. Song

Chonnam National University, Institute for Universe and Elementary Particles, Kwangju, Republic of Korea

S. Choi, D. Gyun, B. Hong, M. Jo, H. Kim, Y. Kim, B. Lee, K.S. Lee, S.K. Park, Y. Roh

Korea University, Seoul, Republic of Korea

M. Choi, J.H. Kim, I.C. Park, S. Park, G. Ryu, M.S. Ryu

University of Seoul, Seoul, Republic of Korea

Y. Choi, Y.K. Choi, J. Goh, E. Kwon, J. Lee, H. Seo, I. Yu

Sungkyunkwan University, Suwon, Republic of Korea

A. Juodagalvis

Vilnius University, Vilnius, Lithuania

J.R. Komaragiri

National Centre for Particle Physics, Universiti Malaya, Kuala Lumpur, Malaysia

H. Castilla-Valdez, E. De La Cruz-Burelo, I. Heredia-de La Cruz ³⁰, R. Lopez-Fernandez, A. Sanchez-Hernandez

Centro de Investigacion y de Estudios Avanzados del IPN, Mexico City, Mexico

S. Carrillo Moreno, F. Vazquez Valencia

Universidad Iberoamericana, Mexico City, Mexico

I. Pedraza, H.A. Salazar Ibarguen

Benemerita Universidad Autonoma de Puebla, Puebla, Mexico

E. Casimiro Linares, A. Morelos Pineda

Universidad Autónoma de San Luis Potosí, San Luis Potosí, Mexico

D. Krofcheck

University of Auckland, Auckland, New Zealand

P.H. Butler, S. Reucroft

University of Canterbury, Christchurch, New Zealand

A. Ahmad, M. Ahmad, Q. Hassan, H.R. Hoorani, S. Khalid, W.A. Khan, T. Khurshid, M.A. Shah, M. Shoib

National Centre for Physics, Quaid-I-Azam University, Islamabad, Pakistan

H. Bialkowska, M. Bluj, B. Boimska, T. Frueboes, M. Górska, M. Kazana, K. Nawrocki, K. Romanowska-Rybinska, M. Szleper, P. Zalewski

National Centre for Nuclear Research, Swierk, Poland

G. Brona, K. Bunkowski, M. Cwiok, W. Dominik, K. Doroba, A. Kalinowski, M. Konecki, J. Krolikowski, M. Misiura, M. Olszewski, W. Wolszczak

Institute of Experimental Physics, Faculty of Physics, University of Warsaw, Warsaw, Poland

P. Bargassa, C. Beirão Da Cruz E Silva, P. Faccioli, P.G. Ferreira Parracho, M. Gallinaro, F. Nguyen, J. Rodrigues Antunes, J. Seixas, J. Varela, P. Vischia

Laboratório de Instrumentação e Física Experimental de Partículas, Lisboa, Portugal

I. Golutvin, V. Karjavin, V. Konoplyanikov, V. Korenkov, G. Kozlov, A. Lanev, A. Malakhov, V. Matveev³¹, V.V. Mitsyn, P. Moisenz, V. Palichik, V. Perelygin, S. Shmatov, S. Shulha, N. Skatchkov, V. Smirnov, E. Tikhonenko, A. Zarubin

Joint Institute for Nuclear Research, Dubna, Russia

V. Golovtsov, Y. Ivanov, V. Kim³², P. Levchenko, V. Murzin, V. Oreshkin, I. Smirnov, V. Sulimov, L. Uvarov, S. Vavilov, A. Vorobyev, An. Vorobyyev

Petersburg Nuclear Physics Institute, Gatchina (St. Petersburg), Russia

Yu. Andreev, A. Dermenev, S. Glinenko, N. Golubev, M. Kirsanov, N. Krasnikov, A. Pashenkov, D. Tlisov, A. Toropin

Institute for Nuclear Research, Moscow, Russia

V. Epshteyn, V. Gavrilov, N. Lychkovskaya, V. Popov, G. Safronov, S. Semenov, A. Spiridonov, V. Stolin, E. Vlasov, A. Zhokin

Institute for Theoretical and Experimental Physics, Moscow, Russia

V. Andreev, M. Azarkin, I. Dremin, M. Kirakosyan, A. Leonidov, G. Mesyats, S.V. Rusakov, A. Vinogradov

P.N. Lebedev Physical Institute, Moscow, Russia

A. Belyaev, E. Boos, V. Bunichev, M. Dubinin⁷, L. Dudko, A. Ershov, V. Klyukhin, O. Kodolova, I. Lokhtin, S. Obraztsov, S. Petrushanko, V. Savrin, A. Snigirev

Skobeltsyn Institute of Nuclear Physics, Lomonosov Moscow State University, Moscow, Russia

I. Azhgirey, I. Bayshev, S. Bitioukov, V. Kachanov, A. Kalinin, D. Konstantinov, V. Krychkine, V. Petrov, R. Ryutin, A. Sobol, L. Tourtchanovitch, S. Troshin, N. Tyurin, A. Uzunian, A. Volkov

State Research Center of Russian Federation, Institute for High Energy Physics, Protvino, Russia

P. Adzic³³, M. Dordevic, M. Ekmedzic, J. Milosevic

University of Belgrade, Faculty of Physics and Vinca Institute of Nuclear Sciences, Belgrade, Serbia

J. Alcaraz Maestre, C. Battilana, E. Calvo, M. Cerrada, M. Chamizo Llatas², N. Colino, B. De La Cruz, A. Delgado Peris, D. Domínguez Vázquez, A. Escalante Del Valle, C. Fernandez Bedoya, J.P. Fernández Ramos, J. Flix, M.C. Fouz, P. Garcia-Abia, O. Gonzalez Lopez, S. Goy Lopez, J.M. Hernandez, M.I. Josa, G. Merino, E. Navarro De Martino, A. Pérez-Calero Yzquierdo, J. Puerta Pelayo, A. Quintario Olmeda, I. Redondo, L. Romero, M.S. Soares

Centro de Investigaciones Energéticas Medioambientales y Tecnológicas (CIEMAT), Madrid, Spain

C. Albajar, J.F. de Trocóniz, M. Missiroli

Universidad Autónoma de Madrid, Madrid, Spain

H. Brun, J. Cuevas, J. Fernandez Menendez, S. Folgueras, I. Gonzalez Caballero, L. Lloret Iglesias

Universidad de Oviedo, Oviedo, Spain

J.A. Brochero Cifuentes, I.J. Cabrillo, A. Calderon, J. Duarte Campderros, M. Fernandez, G. Gomez, A. Graziano, A. Lopez Virto, J. Marco, R. Marco, C. Martinez Rivero, F. Matorras, F.J. Munoz Sanchez, J. Piedra Gomez, T. Rodrigo, A.Y. Rodríguez-Marrero, A. Ruiz-Jimeno, L. Scodellaro, I. Vila, R. Vilar Cortabitarte

Instituto de Física de Cantabria (IFCA), CSIC-Universidad de Cantabria, Santander, Spain

D. Abbaneo, E. Auffray, G. Auzinger, M. Bachtis, P. Baillon, A.H. Ball, D. Barney, A. Benaglia, J. Bendavid, L. Benhabib, J.F. Benitez, C. Bernet⁸, G. Bianchi, P. Bloch, A. Bocci, A. Bonato, O. Bondu, C. Botta, H. Breuker, T. Camporesi, G. Cerminara, T. Christiansen, S. Colafranceschi³⁴, M. D'Alfonso, D. d'Enterria, A. Dabrowski, A. David, F. De Guio, A. De Roeck, S. De Visscher, M. Dobson, N. Dupont-Sagorin, A. Elliott-Peisert, J. Eugster, G. Franzoni, W. Funk, M. Giffels, D. Gigi, K. Gill, D. Giordano, M. Girone, F. Glege, R. Guida, S. Gundacker, M. Guthoff, J. Hammer, M. Hansen, P. Harris, J. Hegeman, V. Innocente, P. Janot, K. Kousouris, K. Krajczar, P. Lecoq, C. Lourenço, N. Magini, L. Malgeri, M. Mannelli, L. Masetti, F. Meijers, S. Mersi, E. Meschi, F. Moortgat, S. Morovic, M. Mulders, P. Musella, L. Orsini, L. Pape, E. Perez, L. Perrozzi, A. Petrilli, G. Petrucciani, A. Pfeiffer, M. Pierini, M. Pimiä, D. Piparo, M. Plagge, A. Racz, G. Rolandi³⁵, M. Rovere, H. Sakulin, C. Schäfer, C. Schwick, S. Sekmen, A. Sharma, P. Siegrist, P. Silva, M. Simon, P. Sphicas³⁶, D. Spiga, J. Steggemann, B. Stieger, M. Stoye, D. Treille, A. Tsirou, G.I. Veres¹⁹, J.R. Vlimant, N. Wardle, H.K. Wöhri, W.D. Zeuner

CERN, European Organization for Nuclear Research, Geneva, Switzerland

W. Bertl, K. Deiters, W. Erdmann, R. Horisberger, Q. Ingram, H.C. Kaestli, S. König, D. Kotlinski, U. Langenegger, D. Renker, T. Rohe

Paul Scherrer Institut, Villigen, Switzerland

F. Bachmair, L. Bäni, L. Bianchini, P. Bortignon, M.A. Buchmann, B. Casal, N. Chanon, A. Deisher, G. Dissertori, M. Dittmar, M. Donegà, M. Dünser, P. Eller, C. Grab, D. Hits, W. Lustermann, B. Mangano, A.C. Marini, P. Martinez Ruiz del Arbol, D. Meister, N. Mohr, C. Nägeli³⁷, P. Nef, F. Nessi-Tedaldi, F. Pandolfi, F. Pauss, M. Peruzzi, M. Quittnat, L. Rebane, F.J. Ronga, M. Rossini, A. Starodumov³⁸, M. Takahashi, K. Theofilatos, R. Wallny, H.A. Weber

Institute for Particle Physics, ETH Zurich, Zurich, Switzerland

C. Amsler³⁹, M.F. Canelli, V. Chiochia, A. De Cosa, A. Hinzmann, T. Hreus, M. Ivova Rikova, B. Kilminster, B. Millan Mejias, J. Ngadiuba, P. Robmann, H. Snoek, S. Taroni, M. Verzetti, Y. Yang

Universität Zürich, Zurich, Switzerland

M. Cardaci, K.H. Chen, C. Ferro, C.M. Kuo, W. Lin, Y.J. Lu, R. Volpe, S.S. Yu

National Central University, Chung-Li, Taiwan

P. Chang, Y.H. Chang, Y.W. Chang, Y. Chao, K.F. Chen, P.H. Chen, C. Dietz, U. Grundler, W.-S. Hou, K.Y. Kao, Y.J. Lei, Y.F. Liu, R.-S. Lu, D. Majumder, E. Petrakou, X. Shi, Y.M. Tzeng, R. Wilken

National Taiwan University (NTU), Taipei, Taiwan

B. Asavapibhop, N. Srimanobhas, N. Suwonjandee

Chulalongkorn University, Bangkok, Thailand

A. Adiguzel, M.N. Bakirci ⁴⁰, S. Cerci ⁴¹, C. Dozen, I. Dumanoglu, E. Eskut, S. Girgis, G. Gokbulut, E. Gurpinar, I. Hos, E.E. Kangal, A. Kayis Topaksu, G. Onengut ⁴², K. Ozdemir, S. Ozturk ⁴⁰, A. Polatoz, K. Sogut ⁴³, D. Sunar Cerci ⁴¹, B. Tali ⁴¹, H. Topakli ⁴⁰, M. Vergili

Cukurova University, Adana, Turkey

I.V. Akin, B. Bilin, S. Bilmis, H. Gamsizkan, G. Karapinar ⁴⁴, K. Ocalan, U.E. Surat, M. Yalvac, M. Zeyrek

Middle East Technical University, Physics Department, Ankara, Turkey

E. Gülmез, B. Isildak ⁴⁵, M. Kaya ⁴⁶, O. Kaya ⁴⁶

Bogazici University, Istanbul, Turkey

H. Bahtiyar ⁴⁷, E. Barlas, K. Cankocak, F.I. Vardarlı, M. Yücel

Istanbul Technical University, Istanbul, Turkey

L. Levchuk, P. Sorokin

National Scientific Center, Kharkov Institute of Physics and Technology, Kharkov, Ukraine

J.J. Brooke, E. Clement, D. Cussans, H. Flacher, R. Frazier, J. Goldstein, M. Grimes, G.P. Heath, H.F. Heath, J. Jacob, L. Kreczko, C. Lucas, Z. Meng, D.M. Newbold ⁴⁸, S. Paramesvaran, A. Poll, S. Senkin, V.J. Smith, T. Williams

University of Bristol, Bristol, United Kingdom

K.W. Bell, A. Belyaev ⁴⁹, C. Brew, R.M. Brown, D.J.A. Cockerill, J.A. Coughlan, K. Harder, S. Harper, E. Olaiya, D. Petyt, C.H. Shepherd-Themistocleous, A. Thea, I.R. Tomalin, W.J. Womersley, S.D. Worm

Rutherford Appleton Laboratory, Didcot, United Kingdom

M. Baber, R. Bainbridge, O. Buchmuller, D. Burton, D. Colling, N. Cripps, M. Cutajar, P. Dauncey, G. Davies, M. Della Negra, P. Dunne, W. Ferguson, J. Fulcher, D. Futyan, A. Gilbert, G. Hall, G. Iles, M. Jarvis, G. Karapostoli, M. Kenzie, R. Lane, R. Lucas ⁴⁸, L. Lyons, A.-M. Magnan, S. Malik, J. Marrouche, B. Mathias, J. Nash, A. Nikitenko ³⁸, J. Pela, M. Pesaresi, K. Petridis, D.M. Raymond, S. Rogerson, A. Rose, C. Seez, P. Sharp [†], A. Tapper, M. Vazquez Acosta, T. Virdee

Imperial College, London, United Kingdom

J.E. Cole, P.R. Hobson, A. Khan, P. Kyberd, D. Leggat, D. Leslie, W. Martin, I.D. Reid, P. Symonds, L. Teodorescu, M. Turner

Brunel University, Uxbridge, United Kingdom

J. Dittmann, K. Hatakeyama, A. Kasmi, H. Liu, T. Scarborough

Baylor University, Waco, USA

O. Charaf, S.I. Cooper, C. Henderson, P. Rumerio

The University of Alabama, Tuscaloosa, USA

A. Avetisyan, T. Bose, C. Fantasia, A. Heister, P. Lawson, C. Richardson, J. Rohlf, D. Sperka, J. St. John, L. Sulak

Boston University, Boston, USA

J. Alimena, S. Bhattacharya, G. Christopher, D. Cutts, Z. Demiragli, A. Ferapontov, A. Garabedian, U. Heintz, S. Jabeen, G. Kukartsev, E. Laird, G. Landsberg, M. Luk, M. Narain, M. Segala, T. Sinthuprasith, T. Speer, J. Swanson

Brown University, Providence, USA

R. Breedon, G. Breto, M. Calderon De La Barca Sanchez, S. Chauhan, M. Chertok, J. Conway, R. Conway, P.T. Cox, R. Erbacher, M. Gardner, W. Ko, R. Lander, T. Miceli, M. Mulhearn, D. Pellett, J. Pilot, F. Ricci-Tam, M. Searle, S. Shalhout, J. Smith, M. Squires, D. Stolp, M. Tripathi, S. Wilbur, R. Yohay

University of California, Davis, Davis, USA

R. Cousins, P. Everaerts, C. Farrell, J. Hauser, M. Ignatenko, G. Rakness, E. Takasugi, V. Valuev, M. Weber

University of California, Los Angeles, USA

J. Babb, R. Clare, J. Ellison, J.W. Gary, G. Hanson, J. Heilman, P. Jandir, E. Kennedy, F. Lacroix, H. Liu, O.R. Long, A. Luthra, M. Malberti, H. Nguyen, A. Shrinivas, J. Sturdy, S. Sumowidagdo, S. Wimpenny

University of California, Riverside, Riverside, USA

W. Andrews, J.G. Branson, G.B. Cerati, S. Cittolin, R.T. D'Agnolo, D. Evans, A. Holzner, R. Kelley, M. Lebourgeois, J. Letts, I. Macneill, D. Olivito, S. Padhi, C. Palmer, M. Pieri, M. Sani, V. Sharma, S. Simon, E. Sudano, M. Tadel, Y. Tu, A. Vartak, F. Würthwein, A. Yagil, J. Yoo

University of California, San Diego, La Jolla, USA

D. Barge, J. Bradmiller-Feld, C. Campagnari, T. Danielson, A. Dishaw, K. Flowers, M. Franco Sevilla, P. Geffert, C. George, F. Golf, J. Incandela, C. Justus, N. Mccoll, J. Richman, D. Stuart, W. To, C. West

University of California, Santa Barbara, Santa Barbara, USA

A. Apresyan, A. Bornheim, J. Bunn, Y. Chen, E. Di Marco, J. Duarte, A. Mott, H.B. Newman, C. Pena, C. Rogan, M. Spiropulu, V. Timciuc, R. Wilkinson, S. Xie, R.Y. Zhu

California Institute of Technology, Pasadena, USA

V. Azzolini, A. Calamba, R. Carroll, T. Ferguson, Y. Iiyama, M. Paulini, J. Russ, H. Vogel, I. Vorobiev

Carnegie Mellon University, Pittsburgh, USA

J.P. Cumalat, B.R. Drell, W.T. Ford, A. Gaz, E. Luiggi Lopez, U. Nauenberg, J.G. Smith, K. Stenson, K.A. Ulmer, S.R. Wagner

University of Colorado at Boulder, Boulder, USA

J. Alexander, A. Chatterjee, J. Chu, S. Dittmer, N. Eggert, W. Hopkins, B. Kreis, N. Mirman, G. Nicolas Kaufman, J.R. Patterson, A. Ryd, E. Salvati, L. Skinnari, W. Sun, W.D. Teo, J. Thom, J. Thompson, J. Tucker, Y. Weng, L. Winstrom, P. Wittich

Cornell University, Ithaca, USA

D. Winn

Fairfield University, Fairfield, USA

S. Abdullin, M. Albrow, J. Anderson, G. Apollinari, L.A.T. Bauerdick, A. Beretvas, J. Berryhill, P.C. Bhat, K. Burkett, J.N. Butler, H.W.K. Cheung, F. Chlebana, S. Cihangir, V.D. Elvira, I. Fisk, J. Freeman,

E. Gottschalk, L. Gray, D. Green, S. Grünendahl, O. Gutsche, J. Hanlon, D. Hare, R.M. Harris, J. Hirschauer, B. Hooberman, S. Jindariani, M. Johnson, U. Joshi, K. Kaadze, B. Klima, S. Kwan, J. Linacre, D. Lincoln, R. Lipton, T. Liu, J. Lykken, K. Maeshima, J.M. Marraffino, V.I. Martinez Outschoorn, S. Maruyama, D. Mason, P. McBride, K. Mishra, S. Mrenna, Y. Musienko³¹, S. Nahn, C. Newman-Holmes, V. O'Dell, O. Prokofyev, E. Sexton-Kennedy, S. Sharma, A. Soha, W.J. Spalding, L. Spiegel, L. Taylor, S. Tkaczyk, N.V. Tran, L. Uplegger, E.W. Vaandering, R. Vidal, A. Whitbeck, J. Whitmore, F. Yang

Fermi National Accelerator Laboratory, Batavia, USA

D. Acosta, P. Avery, D. Bourilkov, M. Carver, T. Cheng, D. Curry, S. Das, M. De Gruttola, G.P. Di Giovanni, R.D. Field, M. Fisher, I.K. Furic, J. Hugon, J. Konigsberg, A. Korytov, T. Kypreos, J.F. Low, K. Matchev, P. Milenovic⁵⁰, G. Mitselmakher, L. Muniz, A. Rinkevicius, L. Shchutska, N. Skhirtladze, M. Snowball, J. Yelton, M. Zakaria

University of Florida, Gainesville, USA

V. Gaultney, S. Hewamanage, S. Linn, P. Markowitz, G. Martinez, J.L. Rodriguez

Florida International University, Miami, USA

T. Adams, A. Askew, J. Bochenek, B. Diamond, J. Haas, S. Hagopian, V. Hagopian, K.F. Johnson, H. Prosper, V. Veeraraghavan, M. Weinberg

Florida State University, Tallahassee, USA

M.M. Baarmand, M. Hohlmann, H. Kalakhety, F. Yumiceva

Florida Institute of Technology, Melbourne, USA

M.R. Adams, L. Apanasevich, V.E. Bazterra, D. Berry, R.R. Betts, I. Bucinskaite, R. Cavanaugh, O. Evdokimov, L. Gauthier, C.E. Gerber, D.J. Hofman, S. Khalatyan, P. Kurt, D.H. Moon, C. O'Brien, C. Silkworth, P. Turner, N. Varelas

University of Illinois at Chicago (UIC), Chicago, USA

E.A. Albayrak⁴⁷, B. Bilki⁵¹, W. Clarida, K. Dilsiz, F. Duru, M. Haytmyradov, J.-P. Merlo, H. Mermerkaya⁵², A. Mestvirishvili, A. Moeller, J. Nachtman, H. Ogul, Y. Onel, F. Ozok⁴⁷, A. Penzo, R. Rahmat, S. Sen, P. Tan, E. Tiras, J. Wetzel, T. Yetkin⁵³, K. Yi

The University of Iowa, Iowa City, USA

B.A. Barnett, B. Blumenfeld, S. Bolognesi, D. Fehling, A.V. Gritsan, P. Maksimovic, C. Martin, M. Swartz

Johns Hopkins University, Baltimore, USA

P. Baringer, A. Bean, G. Benelli, C. Bruner, J. Gray, R.P. Kenny III, M. Murray, D. Noonan, S. Sanders, J. Sekaric, R. Stringer, Q. Wang, J.S. Wood

The University of Kansas, Lawrence, USA

A.F. Barfuss, I. Chakaberia, A. Ivanov, S. Khalil, M. Makouski, Y. Maravin, L.K. Saini, S. Shrestha, I. Svintradze

Kansas State University, Manhattan, USA

J. Gronberg, D. Lange, F. Rebassoo, D. Wright

Lawrence Livermore National Laboratory, Livermore, USA

A. Baden, B. Calvert, S.C. Eno, J.A. Gomez, N.J. Hadley, R.G. Kellogg, T. Kolberg, Y. Lu, M. Marionneau, A.C. Mignerey, K. Pedro, A. Skuja, M.B. Tonjes, S.C. Tonwar

University of Maryland, College Park, USA

A. Apyan, R. Barbieri, G. Bauer, W. Busza, I.A. Cali, M. Chan, L. Di Matteo, V. Dutta, G. Gomez Ceballos, M. Goncharov, D. Gulhan, M. Klute, Y.S. Lai, Y.-J. Lee, A. Levin, P.D. Luckey, T. Ma, C. Paus, D. Ralph, C. Roland, G. Roland, G.S.F. Stephans, F. Stöckli, K. Sumorok, D. Velicanu, J. Veverka, B. Wyslouch, M. Yang, M. Zanetti, V. Zhukova

Massachusetts Institute of Technology, Cambridge, USA

B. Dahmes, A. De Benedetti, A. Gude, S.C. Kao, K. Klapoetke, Y. Kubota, J. Mans, N. Pastika, R. Rusack, A. Singovsky, N. Tambe, J. Turkewitz

University of Minnesota, Minneapolis, USA

J.G. Acosta, S. Oliveros

University of Mississippi, Oxford, USA

E. Avdeeva, K. Bloom, S. Bose, D.R. Claes, A. Dominguez, R. Gonzalez Suarez, J. Keller, D. Knowlton, I. Kravchenko, J. Lazo-Flores, S. Malik, F. Meier, G.R. Snow

University of Nebraska-Lincoln, Lincoln, USA

J. Dolen, A. Godshalk, I. Iashvili, A. Kharchilava, A. Kumar, S. Rappoccio

State University of New York at Buffalo, Buffalo, USA

G. Alverson, E. Barberis, D. Baumgartel, M. Chasco, J. Haley, A. Massironi, D.M. Morse, D. Nash, T. Orimoto, D. Trocino, D. Wood, J. Zhang

Northeastern University, Boston, USA

K.A. Hahn, A. Kubik, N. Mucia, N. Odell, B. Pollack, A. Pozdnyakov, M. Schmitt, S. Stoynev, K. Sung, M. Velasco, S. Won

Northwestern University, Evanston, USA

A. Brinkerhoff, K.M. Chan, A. Drozdetskiy, M. Hildreth, C. Jessop, D.J. Karmgard, N. Kellams, K. Lannon, W. Luo, S. Lynch, N. Marinelli, T. Pearson, M. Planer, R. Ruchti, N. Valls, M. Wayne, M. Wolf, A. Woodard

University of Notre Dame, Notre Dame, USA

L. Antonelli, J. Brinson, B. Bylsma, L.S. Durkin, S. Flowers, C. Hill, R. Hughes, K. Kotov, T.Y. Ling, D. Puigh, M. Rodenburg, G. Smith, C. Vuosalo, B.L. Winer, H. Wolfe, H.W. Wulsin

The Ohio State University, Columbus, USA

E. Berry, O. Driga, P. Elmer, P. Hebda, A. Hunt, S.A. Koay, P. Lujan, D. Marlow, T. Medvedeva, M. Mooney, J. Olsen, P. Piroué, X. Quan, H. Saka, D. Stickland², C. Tully, J.S. Werner, S.C. Zenz, A. Zuranski

Princeton University, Princeton, USA

E. Brownson, H. Mendez, J.E. Ramirez Vargas

University of Puerto Rico, Mayaguez, USA

E. Alagoz, V.E. Barnes, D. Benedetti, G. Bolla, D. Bortoletto, M. De Mattia, A. Everett, Z. Hu, M.K. Jha, M. Jones, K. Jung, M. Kress, N. Leonardo, D. Lopes Pegna, V. Maroussov, P. Merkel, D.H. Miller, N. Neumeister, B.C. Radburn-Smith, I. Shipsey, D. Silvers, A. Svyatkovskiy, F. Wang, W. Xie, L. Xu, H.D. Yoo, J. Zablocki, Y. Zheng

Purdue University, West Lafayette, USA

N. Parashar, J. Stupak

Purdue University Calumet, Hammond, USA

A. Adair, B. Akgun, K.M. Ecklund, F.J.M. Geurts, W. Li, B. Michlin, B.P. Padley, R. Redjimi, J. Roberts, J. Zabel

Rice University, Houston, USA

B. Betchart, A. Bodek, R. Covarelli, P. de Barbaro, R. Demina, Y. Eshaq, T. Ferbel, A. Garcia-Bellido, P. Goldenzweig, J. Han, A. Harel, A. Khukhunaishvili, D.C. Miner, G. Petrillo, D. Vishnevskiy

University of Rochester, Rochester, USA

R. Ciesielski, L. Demortier, K. Goulianos, G. Lungu, C. Mesropian

The Rockefeller University, New York, USA

S. Arora, A. Barker, J.P. Chou, C. Contreras-Campana, E. Contreras-Campana, D. Duggan, D. Ferencek, Y. Gershtein, R. Gray, E. Halkiadakis, D. Hidas, A. Lath, S. Panwalkar, M. Park, R. Patel, V. Rekovic, S. Salur, S. Schnetzer, C. Seitz, S. Somalwar, R. Stone, S. Thomas, P. Thomassen, M. Walker

Rutgers, The State University of New Jersey, Piscataway, USA

K. Rose, S. Spanier, A. York

University of Tennessee, Knoxville, USA

O. Bouhali⁵⁴, R. Eusebi, W. Flanagan, J. Gilmore, T. Kamon⁵⁵, V. Khotilovich, V. Krutelyov, R. Montalvo, I. Osipenkov, Y. Pakhotin, A. Perloff, J. Roe, A. Rose, A. Safonov, T. Sakuma, I. Suarez, A. Tatarinov

Texas A&M University, College Station, USA

N. Akchurin, C. Cowden, J. Damgov, C. Dragoiu, P.R. Dudero, J. Faulkner, K. Kovitanggoon, S. Kunori, S.W. Lee, T. Libeiro, I. Volobouev

Texas Tech University, Lubbock, USA

E. Appelt, A.G. Delannoy, S. Greene, A. Gurrola, W. Johns, C. Maguire, Y. Mao, A. Melo, M. Sharma, P. Sheldon, B. Snook, S. Tuo, J. Velkovska

Vanderbilt University, Nashville, USA

M.W. Arenton, S. Boutle, B. Cox, B. Francis, J. Goodell, R. Hirosky, A. Ledovskoy, H. Li, C. Lin, C. Neu, J. Wood

University of Virginia, Charlottesville, USA

S. Gollapinni, R. Harr, P.E. Karchin, C. Kottachchi Kankanamge Don, P. Lamichhane

Wayne State University, Detroit, USA

D.A. Belknap, D. Carlsmith, M. Cepeda, S. Dasu, S. Duric, E. Friis, R. Hall-Wilton, M. Herndon, A. Hervé, P. Klabbers, J. Klukas, A. Lanaro, C. Lazaridis, A. Levine, R. Loveless, A. Mohapatra, I. Ojalvo, T. Perry, G.A. Pierro, G. Polese, I. Ross, T. Sarangi, A. Savin, W.H. Smith, N. Woods

University of Wisconsin, Madison, USA

[†] Deceased.

¹ Also at Vienna University of Technology, Vienna, Austria.

² Also at CERN, European Organization for Nuclear Research, Geneva, Switzerland.

³ Also at Institut Pluridisciplinaire Hubert Curien, Université de Strasbourg, Université de Haute Alsace Mulhouse, CNRS/IN2P3, Strasbourg, France.

⁴ Also at National Institute of Chemical Physics and Biophysics, Tallinn, Estonia.

⁵ Also at Skobeltsyn Institute of Nuclear Physics, Lomonosov Moscow State University, Moscow, Russia.

⁶ Also at Universidade Estadual de Campinas, Campinas, Brazil.

⁷ Also at California Institute of Technology, Pasadena, USA.

⁸ Also at Laboratoire Leprince-Ringuet, Ecole Polytechnique, IN2P3-CNRS, Palaiseau, France.

⁹ Also at Suez University, Suez, Egypt.

¹⁰ Also at Cairo University, Cairo, Egypt.

- ¹¹ Also at Fayoum University, El-Fayoum, Egypt.
- ¹² Also at British University in Egypt, Cairo, Egypt.
- ¹³ Now at Ain Shams University, Cairo, Egypt.
- ¹⁴ Also at Université de Haute Alsace, Mulhouse, France.
- ¹⁵ Also at Joint Institute for Nuclear Research, Dubna, Russia.
- ¹⁶ Also at Brandenburg University of Technology, Cottbus, Germany.
- ¹⁷ Also at The University of Kansas, Lawrence, USA.
- ¹⁸ Also at Institute of Nuclear Research ATOMKI, Debrecen, Hungary.
- ¹⁹ Also at Eötvös Loránd University, Budapest, Hungary.
- ²⁰ Also at University of Debrecen, Debrecen, Hungary.
- ²¹ Now at King Abdulaziz University, Jeddah, Saudi Arabia.
- ²² Also at University of Visva-Bharati, Santiniketan, India.
- ²³ Also at University of Ruhuna, Matara, Sri Lanka.
- ²⁴ Also at Isfahan University of Technology, Isfahan, Iran.
- ²⁵ Also at Sharif University of Technology, Tehran, Iran.
- ²⁶ Also at Plasma Physics Research Center, Science and Research Branch, Islamic Azad University, Tehran, Iran.
- ²⁷ Also at Università degli Studi di Siena, Siena, Italy.
- ²⁸ Also at Centre National de la Recherche Scientifique (CNRS) – IN2P3, Paris, France.
- ²⁹ Also at Purdue University, West Lafayette, USA.
- ³⁰ Also at Universidad Michoacana de San Nicolas de Hidalgo, Morelia, Mexico.
- ³¹ Also at Institute for Nuclear Research, Moscow, Russia.
- ³² Also at St. Petersburg State Polytechnical University, St. Petersburg, Russia.
- ³³ Also at Faculty of Physics, University of Belgrade, Belgrade, Serbia.
- ³⁴ Also at Facoltà Ingegneria, Università di Roma, Roma, Italy.
- ³⁵ Also at Scuola Normale e Sezione dell'INFN, Pisa, Italy.
- ³⁶ Also at University of Athens, Athens, Greece.
- ³⁷ Also at Paul Scherrer Institut, Villigen, Switzerland.
- ³⁸ Also at Institute for Theoretical and Experimental Physics, Moscow, Russia.
- ³⁹ Also at Albert Einstein Center for Fundamental Physics, Bern, Switzerland.
- ⁴⁰ Also at Gaziosmanpasa University, Tokat, Turkey.
- ⁴¹ Also at Adiyaman University, Adiyaman, Turkey.
- ⁴² Also at Cag University, Mersin, Turkey.
- ⁴³ Also at Mersin University, Mersin, Turkey.
- ⁴⁴ Also at Izmir Institute of Technology, Izmir, Turkey.
- ⁴⁵ Also at Ozyegin University, Istanbul, Turkey.
- ⁴⁶ Also at Kafkas University, Kars, Turkey.
- ⁴⁷ Also at Mimar Sinan University, Istanbul, Istanbul, Turkey.
- ⁴⁸ Also at Rutherford Appleton Laboratory, Didcot, United Kingdom.
- ⁴⁹ Also at School of Physics and Astronomy, University of Southampton, Southampton, United Kingdom.
- ⁵⁰ Also at University of Belgrade, Faculty of Physics and Vinca Institute of Nuclear Sciences, Belgrade, Serbia.
- ⁵¹ Also at Argonne National Laboratory, Argonne, USA.
- ⁵² Also at Erzincan University, Erzincan, Turkey.
- ⁵³ Also at Yildiz Technical University, Istanbul, Turkey.
- ⁵⁴ Also at Texas A&M University at Qatar, Doha, Qatar.
- ⁵⁵ Also at Kyungpook National University, Daegu, Republic of Korea.

Update

Physics Letters B

Volume 757, Issue , 10 June 2016, Page 569

DOI: <https://doi.org/10.1016/j.physletb.2016.04.010>



Corrigendum

Corrigendum to “Measurement of the $pp \rightarrow ZZ$ production cross section and constraints on anomalous triple gauge couplings in four-lepton final states at $\sqrt{s} = 8$ TeV” [Phys. Lett. B 740 (2015) 250]

CMS Collaboration*

CERN, Switzerland

ARTICLE INFO

Article history:

Available online 8 April 2016

Keywords:

CMS
Physics
Electroweak

An error was found in the published version in the right plot in Fig. 4. The bin-by-bin normalization for data and MC prediction in this plot is incorrect. The corrected figure is shown in Fig. 1. The physics conclusion of the paper remains unchanged.

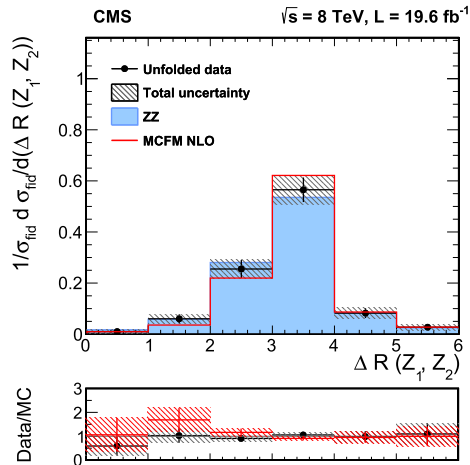


Fig. 1. Differential cross section normalized to the fiducial cross section for the combined $4e$, 4μ , and $2e2\mu$ decay channels as a function of ΔR between the Z -bosons. Points represent the data, and the shaded histograms labeled ZZ represent the POWHEG+GG2ZZ+PYTHIA predictions for ZZ signal, while the solid curve corresponds to results of the MCFM calculations. The bottom part represents the ratio of the measured cross section to the expected one from POWHEG+GG2ZZ+PYTHIA (black crosses with solid symbols) and MCFM (red crosses). The shaded areas on all the plots represent the full uncertainties calculated as the quadrature sum of the statistical and systematic uncertainties, whereas the crosses represent the statistical uncertainties only. (For interpretation of the references to color in this figure legend, the reader is referred to the web version of this article.)

DOI of original article: <http://dx.doi.org/10.1016/j.physletb.2014.11.059>.* E-mail address: cms-publication-committee-chair@cern.ch (CMS Collaboration).